# ULTRA-WIDEBAND CHANNEL MEASUREMENT AND MODELING FOR UNMANNED AERIAL VEHICLE TO WEARABLE COMMUNICATION

By

SURBHI VISHWAKARMA

Bachelor of Technology in Electronics and

Communication Engineering

Vellore Institute of Technology

Vellore, Tamil Nadu

2015

Submitted to the Faculty of the
Graduate College of the
Oklahoma State University
in partial fulfillment of
the requirements for
the Degree of
MASTER OF SCIENCE
May, 2018

ULTRA-WIDEBAND CHANNEL MEASUREMENT AND MODELING FOR UNMANNED AERIAL VEHICLE TO WEARABLE COMMUNICATION

Thesis Approved:

Dr. Sabit Ekin

**Thesis Adviser**

Dr. James West

**Committee Member**

Dr. Charles Bunting

**Committee Member**

# ACKNOWLEDGEMENTS

I have been fortunate to have Dr. Sabit Ekin as a research supervisor, who has always been very understanding and kept on comforting me towards all the professional and personal issues I faced throughout my MSc program. I have been associated with him from the first semester and feel honored to be his first MSc. student. I have thoroughly enjoyed his constant support, encouragement, prompt responses, innovative ideas and perennial guidance, it definitely eased my master's journey and made it very productive and knowledgeable. He provided proper research methodologies and regardless of any time consideration stood beside me through every single measurement which is present in my thesis. I would like to extend my gratitude towards him for not only providing a healthy and peaceful working environment but also for extending his friendship by providing countless free meals, cookouts, movie sessions, due to which US always felt like home away from home. I would never have given thought about thesis if it would not have been him. Thank you so much for believing in me.

I would like to express my gratitude towards Dr. Qammer H. Abbasi, Professor at the University of Glasgow for his guidance from the baby steps to throughout the Ultra-Wideband methodology. Also, my lab members for their immense contribution of time during my measurement sessions. I would specially like to acknowledge Amit Kachroo and Wesley Caswell for being the best human subject and standing during long measurement sessions. I would like thank to Hisham Abuella, for his help with the MATLAB code. Adithya Popuri, for taking measurement pictures. My work would not have been done without the help of Jacob Dixon, thank you so much for your exceptional help with the python code and the VNA, I truly appreciate it.

Secondly, I would like to thank my thesis committee: Dr. Charles Bunting and Dr. James West for providing access to the Richmond Hill lab and all the support with the measuring instruments. Special thanks to Dr. Jamey Jacob's Unmanned System Research Institute (USRI) lab for providing unmanned aircraft systems.

I would like to thank my friends: Akshay and Anirban, Family: Mom, Dad, Shubham for being my backbone throughout my degree program. Last but not the least, Coco and Zuko for being the most loving and best stress-busting dogs.

Name: SURBHI VISHWAKARMA

Date of Degree: MAY, 2018

Title of Study: ULTRA-WIDEBAND CHANNEL MEASUREMENT AND MODELING FOR UNMANNED AERIAL VEHICLE TO WEARABLE COMMUNICATION

Major Field: ELECTRICAL ENGINEERING

**Abstract**: Ultra-Wideband (UWB) has impacted our lives in impressive ways, it is one of the high potential areas with enormous benefits, especially for the short-range communication. With more discoveries, technology changed and the importance of wideband network was favored over narrowband. Officially, in the year 1933, Armstrong found and recognized the advantages of wideband signaling. Later, UWB was coined and took a fast pace and changed the conduct of the society in many ways. The most significant part about UWB is its applications, one of the claims i.e., Off-body is thoroughly studied and analyzed throughout the thesis.

We performed one of the first vertical link channel studies with Off-body channel characterization with one UWB antenna patch on Unmanned Aerial Vehicle (UAV) and another antenna at different body locations on a real human subject for the frequency bandwidth of 3.1-10.6 GHz in different environments such as anechoic, indoor, and outdoor. The main purpose is to monitor how UWB system is affected by both large and small-scale fading, that's why it was worth taking measurements in all three settings for the analysis. Also, it was critical to pick one best distributions among Lognormal, Rayleigh, Nakagami, Normal, Weibull, Gamma, Exponential and Rician using Akaike Information Criteria (AIC). The path loss varies in different environments, and its exponent becomes important parameter to be determined for all three settings.

It was interesting to study how UWB characteristics varied with different environments. The delay profiles such as power delay profile (PDP), root mean square (RMS), maximum excess and mean excess delays were analyzed. For all the analysis, we used two small, light weighted compatible antenna patches, which supported UWB bandwidth and consumed less power so that it could be safely attached to a human body.

Our work is mainly focused on the detailed understanding of standard UWB path loss and delay spreads for the communication channel between UAV and wearable. We believe this study would help us in understanding UWB Off body characteristics thoroughly and would also help in health monitoring and improvising the optimum location of the human body tag.

TABLE OF CONTENTS

Chapter Page

LIST OF TABLES

Table Page

LIST OF FIGURES

Figure Page

# CHAPTER I

## INTRODUCTION

"*When wireless is perfectly applied the whole earth will be converted into a huge brain.*"

-Nikola Tesla

In contemporary world, we are surrounded by wireless systems from headsets to automobile, everything is functioning wirelessly. There was a time when thinking about communicating with a person sitting in a different country was a dream, however, with time now what we see is conversing with anyone, anywhere smoothly; definitely, wireless has pushed our boundaries and helped our society in achieving unimaginable. Especially, in past ten years, the growth of communications industry has manifolded, integration has been on a large scale and has given rise to miniature technologies, which has made wireless economical and reliable [38]. Today, from entertainment to transferring highly secured data, wireless is being trusted in spite of having many limitations.

Wireless has been chosen because of its convenience over other network types and with years passing by it has undoubtedly brought all great inventions, which has led wireless to be the fastest growing segment of the communication industry [39]. When the wireless communication was naive to the existence it was used for narrowed down bandwidths, with even little broad bands there were high chances of getting noise added to the system. In addition, previously not all the devices were compatible with the wideband area networks; hence mostly narrowband existed and the products which could support narrow bandwidths. With the expansion of wideband  came the existence of

many technologies, along with the other ones came UWB technology. The brief history of UWB is shown in Figure 1.1. The name UWB coined because of its extensive bandwidth of up to 7.5 Gbps, which was undoubtedly huge. Any system was categorized as UWB when the absolute bandwidth was more than 500 MHz [22], and still, we follow the same definition.

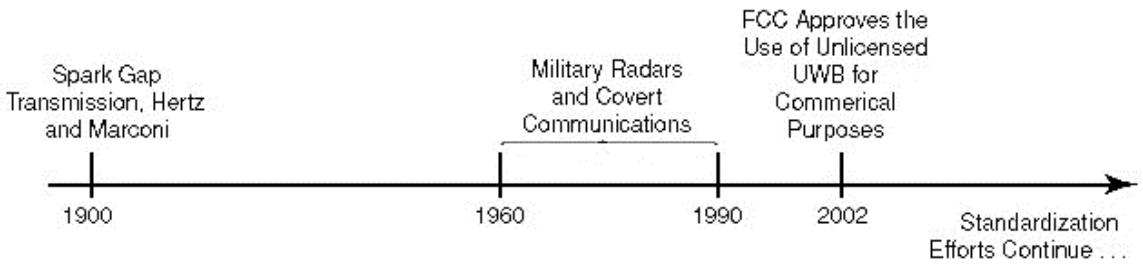


Figure 1.1 A brief history of UWB communication [30].

UWB is a type of radio; it is not exactly a conventional kind of radio system. As we are familiar, radio is a technology in which EM waves could be sent or received using a Transmitter and a Receiver, which is shown in the Figure 1.2.

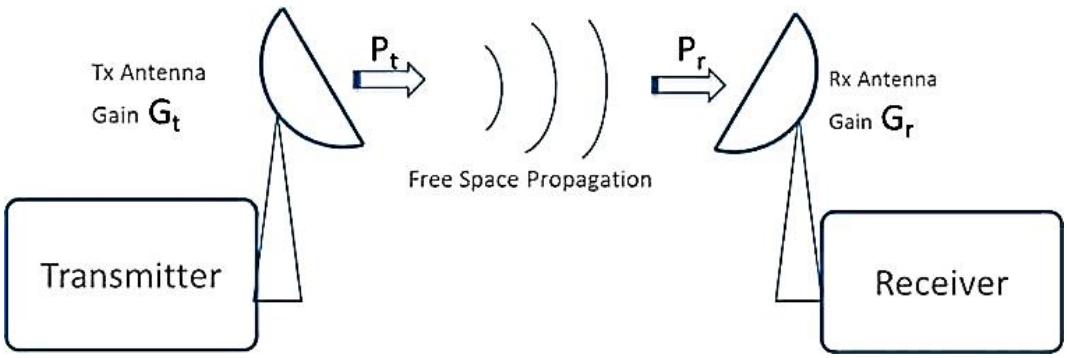


Figure 1.2 A basic radio system with transmitter, propagation medium and receiver [40].

Radio is used for transmitting, music, video, voice, telephony or a highly ciphered information,

this information could be keenly observed and read at the end of the receiver. We can tune a particular frequency for listening to music, for watching TV or for making a call to a specific person, everything is possible because of the electromagnetic waves, which are processed through a radio system. When a signal is without information, it is considered to have zero bandwidth. When data is modulated to the message (signal), it expands the information bandwidth [1]. The zero bandwidths represent the narrowband signals.

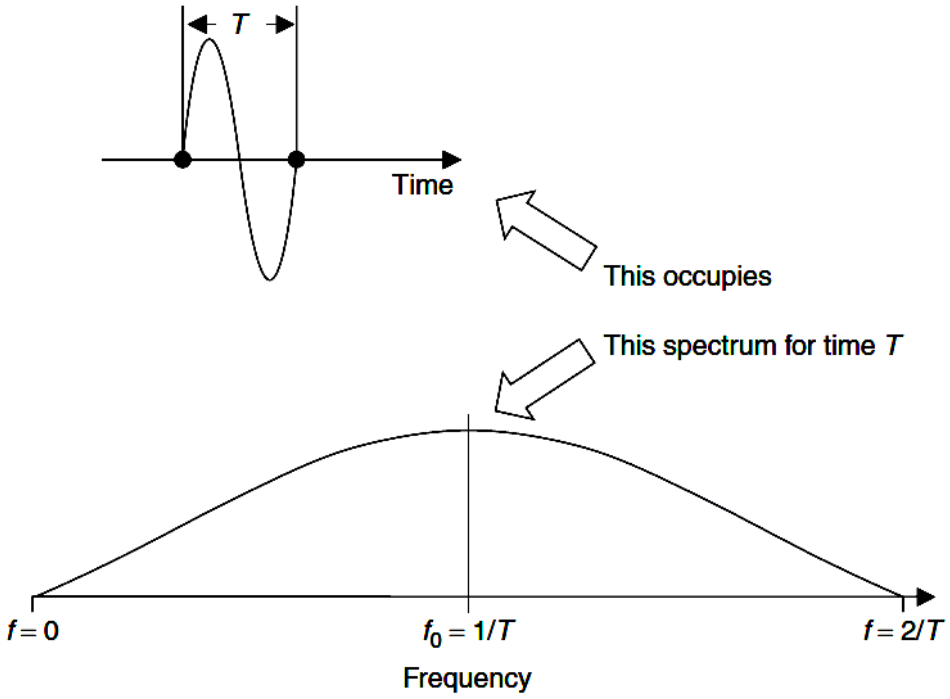


Figure 1.3 The fundamental of UWB [1]

As we can see in the Figure 1.3, a signal with information, when bifurcated using time, especially as a narrow lane of time [1]. Instead of small bandwidth, they occupy broad bands also known as UWB, which give rise to Ultrawideband concept. The UWB signal is defined as the integration of sub-narrowband signals each having a center frequency, which means that the wavelength of the entire UWB signal will change significantly over the whole frequency band [41]. Hence, it is a unique kind of extensive range UWB radio with the FCC approved [29] frequency range of 3.1-

10.6 GHz [24,25]. For deploying UWB based products in the market, Institute of Electrical and Electronics Engineers (IEEE) performed significant work and assigned IEEE 802.15.4a as a standard.

When a signal is modulated, coded and made highly compact with respect to the time but not with the frequency, this fundamental idea is referred as UWB. It has many benefits, one of them is it can accommodate multiple users. Rather than frequency the users are separated using time [1-2]. The best representation of multiple users in time is shown in the Figure 1.4.

UWB has many other advantages which makes it a reliable source. The broad bandwidth of 7.5 GHz and potentially 100 Mbps of the high data rate has application in high-definition television pictures, less of multipath interference and low power hence longer battery life [2-3]. It is also considered beneficial for location-based applications, such as, using wireless networks in a limited area securely, which used the data rate of below 1 Mbps [27]. One of the successful location-based services so far is 911 emergency number [26]. UWB is already used in military applications, and due to its potential, it is expected to have more usage in wireless communication and ranging in future [41]. So far, the unlicensed band of 2.45 GHz was studied for the On-body characterization, but a colossal scope was observed for the UWB which drew the attention of many researchers. UWB On-body radio channel characterization and system level modelling for body-centric wireless networks have been presented extensively in the open literature [3-4, 5–17]. Many researchers in the different areas have studied the UWB channel characterisation for standing and day to day life postures [5-17].

Another advantage of UWB that makes it reliable for both the On-body and Off-body characterisation is the high-frequency bandwidth range. As we know by the mathematical expression of $c = f\lambda$ the frequency and wavelength are inversely proportional to each other. Hence, when the frequency is high, the wavelength associated with it would be short, and a short

wavelength leads to an antenna of small size. The small size of antenna patch is useful for both the types of body characterisations, small size makes it wearable and handy. Similar kind of small patch isotropic antenna was used for our experiment, for obtaining all the measurements.

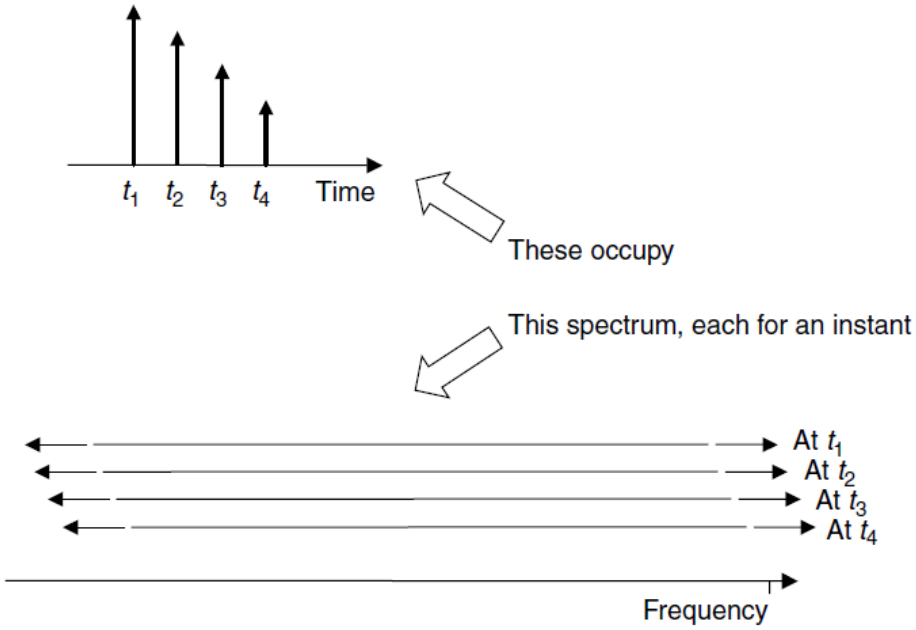


Figure 1.4 Representing the multiple users accommodated in UWB with the time separation [1].

UWB channel has several qualities which could be an exciting finding in the wireless communications, we are interested in body-centric discussion. There are two ways the body channel characterization is performed, one is On-body, and another one is Off-body. Such communication trend dealing with On and Off-body is a hot topic of research [18-20] and also very critical to understand the fundamental difference between both the systems. On-body communication is a system in which both the receiver and transmitter are placed on the human subject. On-body communication is very trendy in the contemporary world, moreover; as a result, there are many health monitoring devices. Today, we can easily keep track of our heartbeat, sugar level, etc. Whereas, Off-body communication is a system in which either the receiver or the

transmitter is attached to the body and whichever is not mounted on the body is kept away from the body at a certain distance. Off-body communication could be either wired or wireless.

One of the best day to day examples of Off-body communication is ECG (electrocardiogram), in which sensors are attached to the human body and the status is observed on the receiver's screen which is not mounted on the subject. Also, NASA uses Off-body method for tracking the health of astronauts using sensors on their spacesuit. In this work, we were keen to study Off-body centric communication using microstrip patch antenna, which is isotropic. We are planning to study the behavior of UWB antenna patch in three different environments, i.e., anechoic chamber, indoor warehouse scenario and outdoor.

For the study of the far field, in each of the three scenarios measurements were taken at different distances ranging 3.5 to 8.0 meters. The basic idea of taking measures in the different environments is to understand the path loss and finding the path loss exponent for each one of them. Once we are familiar with the path loss and its exponent, we found the impulse response for each distance of respective body locations, then based upon the impulse response we ended up analyzing delays such as power delay profile, mean excess delay, maximum excess delay and RMS delay.

## 1.1 RESEARCH OBJECTIVE

The primary objective of the research is to come up with an optimum location for antenna patch on the human body; this would be a helpful study for deciding the best locations for placing sensors on the human body for health monitoring. In our work, we are performing the channel characterization by developing a wireless communication between UAV and wearable device. There are many efficient body based sensors in the market, not all the sensors provide the valid results, many times main reason for the non-effective result is not being able to come up with best sensor location. When two sensors are in the line of sight (LOS) with each other, the system works and monitors the best. However, with non-line of sight (NLOS) the results observed are different, with more body movement the sensor location continually varies with respect to the receiver and hence show continuous variation. It is crucial to study the change because in practical scenario because nothing is stable and with the body movement the sensor location also continuously varies. Hence, we picked the best body locations and analyzed each of the areas at different distances between 3.5 - 8 meters with the interval of 0.5 meters in the anechoic, indoor warehouse and outdoor environment. A significant point to be noted is that we are relying on averaging, which means for each distance we have taken ten different measurements, and for each of the distance point we have found scattering parameter, i.e., $S_{21}$ for the frequency range of 3.1-10.6 GHz, hence we are concerned with the average value of $S_{21}$. The averaged $S_{21}$ is used for finding the path loss exponent using linear regression, we have used Least Squares (LS) method. Also, $S_{21}$ value has been helpful in coming up with the impulse response for each of the distance at different frequencies ranging from 3.1 to 10.6 GHz.

Moreover, in this study, the delay parameters have been investigated as well for coming up with the best sensor location. For coding, we used MATLAB. All the measurements were taken in the environment of Richmond Hill lab, Oklahoma State University, Stillwater.

## 1.2 THESIS ORGANIZATION

The thesis work consists of four chapters, Chapter 1 provides the fundamental introduction of the primary topic, i.e., UWB communication, and explanation of the primary objective of the study. Chapter 2 starts with the discussion of the UWB, we discussed the type of antenna requirement for the measurement and other required equipment, in other sections the UWB antenna behavior has been studied in three environments with varying distances and changing antenna locations. For understanding the propagation of UWB communication, path loss has been characterized for each body channel and respective path loss exponent and time dispersion parameters have been determined. Chapter 3 discusses the changing behavior of UWB with different human postures for LOS and NLOS in the indoor and outdoor environments. In this chapter, again the path loss dependency was compared with the distance, and time dispersion parameters were characterized for different human postures. In Chapter 4, the results are presented based on the analysis of the UWB antenna. Further, the conclusion has been extended to the future work.

CHAPTER 2

# OFF-BODY CHANNEL CHARACTERIZATION FOR DIFFERENT ENVIRONMENT

## 2.1 INTRODUCTION

UWB channel characterizations have been done in many different environments, such as office, house, airplane, outdoor, and underwater. Researchers have been working hard to know all the aspects related to UWB for receiving all the benefits out of it. UWB comes with so many advantages, one of the significant advantages is low power requirements, which make them very comfortable to be placed on any human body type. Also, due to low power, there is minimal noise interference which makes it perfect for short range, high data rate applications [43] and deployable for LOS and NLOS [22]. These advantages make UWB Technology a perfect fit for body-centric communications. Body-centric is one primary field of study these days. Body-centric is a network in which a bunch of low power sensors is spread around the human body to record specified physiological data for healthcare monitoring, and the human body is used as a transmission medium [31,44]. The human body is a complex structure; in body-centric communication, we make sure that signals don't harm the sensitive human body surface, also, don't compromise with the system quality. Luckily, for UWB, Federal Communications Commission (FCC) has defined power requirement as - 41.3 dBm/MHz, or 75 nanowatts/MHz [43] which doesn't have any adverse effect on human body cells.

Body-centric communication are of three types,

- On-body
- Off-body

- In-body

These are very simple networks shown in the Figure 2.1; the On-body communicates when both Transmitter (Tx) and Receiver (Rx) are present on the human body. The Off-body communicates when either transmitter or receiver are present on the human body. The In-body communicates when one of the nodes is implanted inside the human body [42].

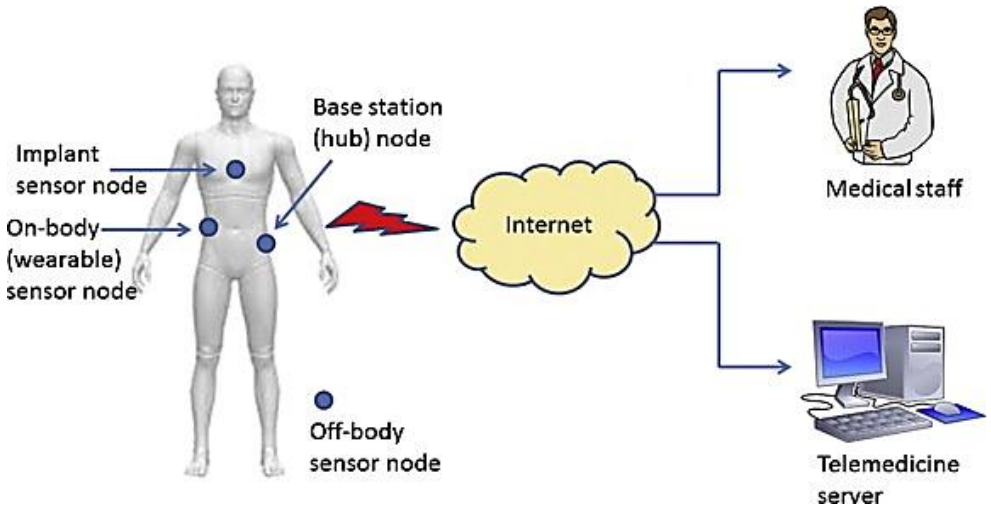


Figure 2.1 Subdomain of body centric communication [37].

UWB has another advantage, due to the high frequency they have the tendency to penetrate most of the materials, which makes them applicable for through-the-walls communication and ground penetrating radars [43]. When any wireless signal travels, there are three basic propagation mechanisms occur, reflection, diffraction, and scattering. Reflection occurs when a signal strikes on an object. Diffraction occurs when a sharp-edged surface obstructs path between transmitter and receiver. Scattering occurs when an object kept in between the path of receiver and transmitter is smaller than the wavelength of the signal. The indoor warehouse and outdoor environment both get affected by all three propagation mechanisms and hence lead to different kinds of fading. Multipath fading is interference between two or more versions of signal arriving at two different times at the receiver [38]. Shadowing occurs due to the obstacles between transmitter and receiver, whereas,

power attenuates due to absorption, reflection, scattering and diffraction [39]. Variation due to shadowing and path loss occurs over large distances referred as large-scale propagation, whereas, multipath occurs at very short distances and referred as small-scale propagation effects. Small scale fading arises due to multipath propagation, speed of receiver and speed of the surrounding objects [38]. Multipath is also known as simple fading, describes the rapid fluctuation of amplitude over short period of time or travel distance and ignores large scale path loss effects [38]. The basic propagation effects are shown in Figure 2.2.

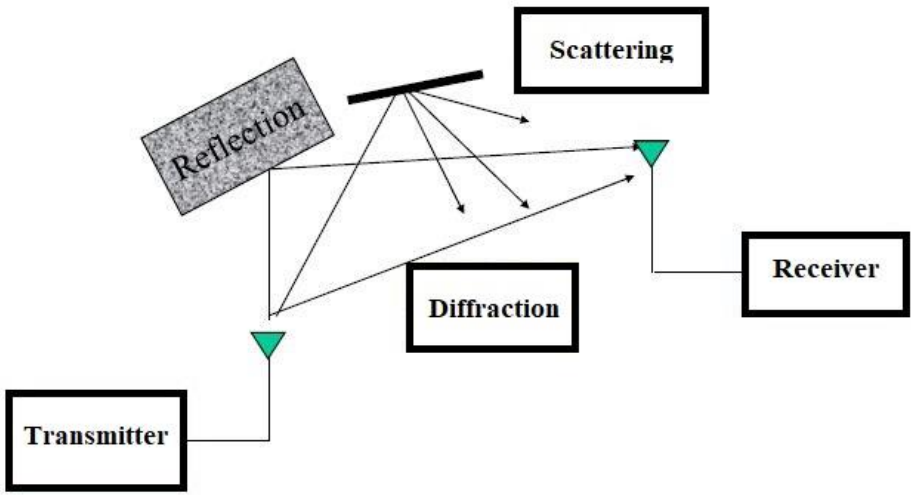


Figure 2.2 The basic propagation mechanism effects.

However, the performance of a UWB communications system is affected due to strong narrowband interference from the radio transmission [43]. It is essential to study the path loss and its exponent because multipath is impossible to avoid in UWB. Although, studies have shown short UWB pulses are not profoundly affected by the multipath but fading affects the system performance strongly, that's why it is strongly recommended to study time dispersion parameters as well. In this work, we are dealing with the Off-body communication. We are interested in UWB Off-body channel characterization, finding path loss with distance-dependency and the time dispersion parameters due to large scale fading.

## 2.2 MEASUREMENT METHODOLOGY

For performing UWB measurement, firstly, it was essential to decide an environment. Once a setting was fixed, the measurements were taken in the frequency domain. We used UWB based sensor which is also referred as a node, for capturing the data from the human body. It consists of nothing but an antenna patch for communicating with the other UWB based sensor which would be located at the certain distance from the human body. As we are performing Off-body characterization, we have to make sure both the sensors should not be on the same human subject. The UWB signal penetrates many materials but due to low power it is not harmful to the humans, for making sure we got the antennas tested. In this work, we have analyzed the antenna patch in three multipath environments and studied the path loss exponent for each one of them.

### 2.2.1. MEASUREMENT SETUP

Before going to the procedure of how to take measurements, it is essential to understand the entire measurement setup correctly. The basic UWB communication system is shown in the Figure 2.3. In our setup the structure is straightforward and consists of;

- Transmitter: The signal is transmitted through one of the UWB patches.
- Receiver: Another UWB patche receive the signal.
- RF coaxial cables: For connecting VNA to the antenna patches. Weight: 2 lbs.
- Calibration kit: Agilent 85032F.
- Vector Network Analyzer (VNA): VNA is test equipment which helps RF and microwave devices to be characterized as scattering parameter also known as S parameters. (Agilent 8722ES [50 MHz- 40 GHz]) [52].

- Data acquisition device: A laptop.

| EQUIPMENT | SPECIFICATIONS |
|---|---|
| Vector Network Analyzer | Agilent 8722ES [50 MHz – 40 GHz ] |
| Calibration kit | Agilent 85032F |
| UAV | 3 DR \| IRIS + Quadcopter |
| RF coaxial cables | Weight ~ 2 lbs |
| 2 Antenna sensors | OctaneBW-3000-10000-EG [3GHz -11 GHz] |

Table 2.1 The measurement equipment and their specifications.

This is a simple setup which explains how the data is transferred from transmitter to the receiver through the propagation channel. Both the transmitter and the receiver are attached to the VNA through the port one and port two respectively. The measurements were performed in the frequency domain using VNA [45]. Finally, the measured data, i.e., frequency responses are acquired through the laptop for analysis. Hence, channel transfer function $H(f) = S_{21}(f)$ is determined.

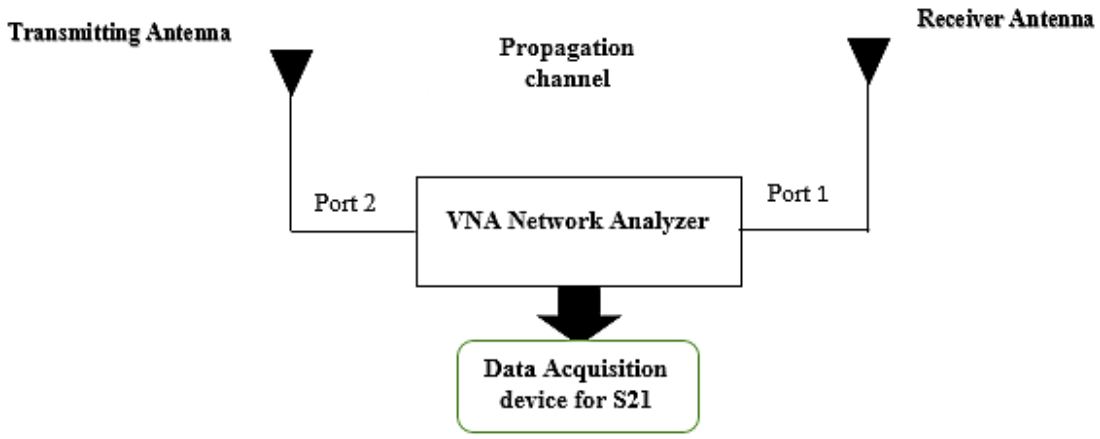


Figure 2.3 The standard block diagram of UWB communication system.

Although in our setup we have a transmitter UWB antenna patch on the UAV and receiver antenna patch on the human subject, which is shown in the Figure 2.4. UAV is used because it helps in providing vertical link communication and complexity to the overall system. The antenna patches

were connected to the VNA via RF coaxial cables of length 3-5 and 10 meters. It was necessary for the setup, having a human subject and his physical details like, height and weight, which in our case was an adult male with height of 1.8 meters and weight of 78 kgs.

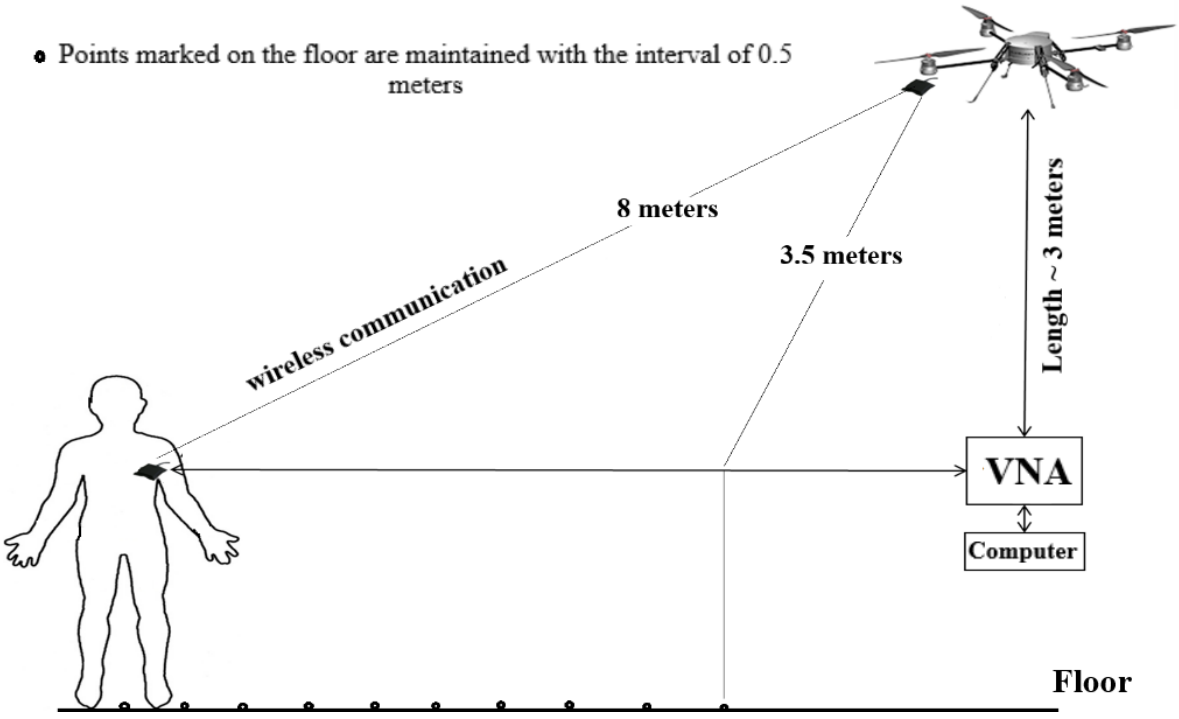


Figure 2.4 The sketch plan of the measurement setup for UWB Off-body characterization.

We started with placing UWB antenna sensor at different body locations to the human subject, forehead, heart, abdomen, right arm / wrist / waist/ thigh / shin. We considered the left side of the human body as well and took measurements for left arm / shin which was surprisingly similar to the measured data results of right arm / shin, because the distance of left and right arm / wrist was identical from the UAV. Hence, instead of spending time on the entire left side of measurement we considered body and data points symmetrical and focused on one side of the body for analysis to save time.

VNA was set with the sweep time of 100 milliseconds (ms), to generate 1601 continuous wave tones those were uniformly distributed over the 3.1-10.6 GHz spectrum [22], with frequency

interval 10 MHz, S-parameter ($S_{21}$) test set to measure the sampled frequency response of the channel [41]. The transmit power level set for VNA was -10dBm. The Figure 2.5 shows the Agilent's VNA setup.

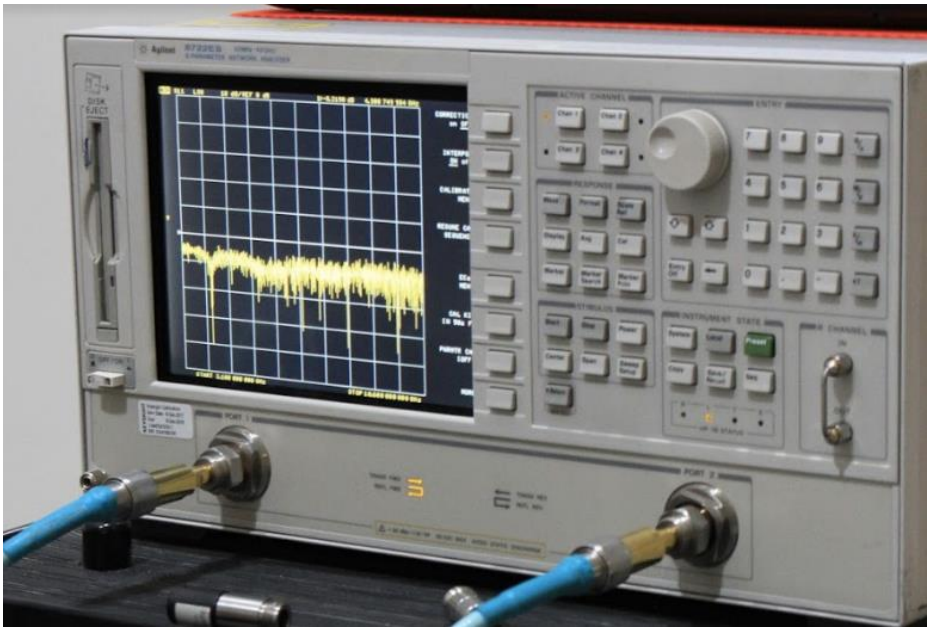

Figure 2.5 The VNA used for the recovering $S_{21}$ parameter.

Antenna characteristics usually affect the radio signal propagation [41]. As we know, UWB occupies broad frequency band, hence, the message is not flat over the frequency. Moreover, picking a right antenna becomes an essential part of the UWB channel. Also, its frequency response changes over the entire bandwidth and the channel impulse response is obtained using the inverse Fourier transform, which we would be studying in coming sections [41]. For both transmission and receiving nodes, we used Octane BW-3000-10000-EG Omni-directional, vertically analyzed, wideband antennas with 5.5 dBi gain @ 3 GHz, 8.2 dBi gain @ 6 GHz and 6.3 dBi gain @ 9 GHz. Antenna made up of flexible material, lightweight (2 ounces), small in size with dimension 4.5″ x 4.25″ x 0.4″ which is shown in the Figure 2.7, and VSWR less than 2:1, the radiation pattern of UWB antenna is given in the Figure 2.6.

The radiation pattern is also known as far field pattern or antenna pattern that represents the directional dependence of the strength of radio waves from antenna. It is basically a graphical representation of the radiation properties of antenna as a function of space coordinates.

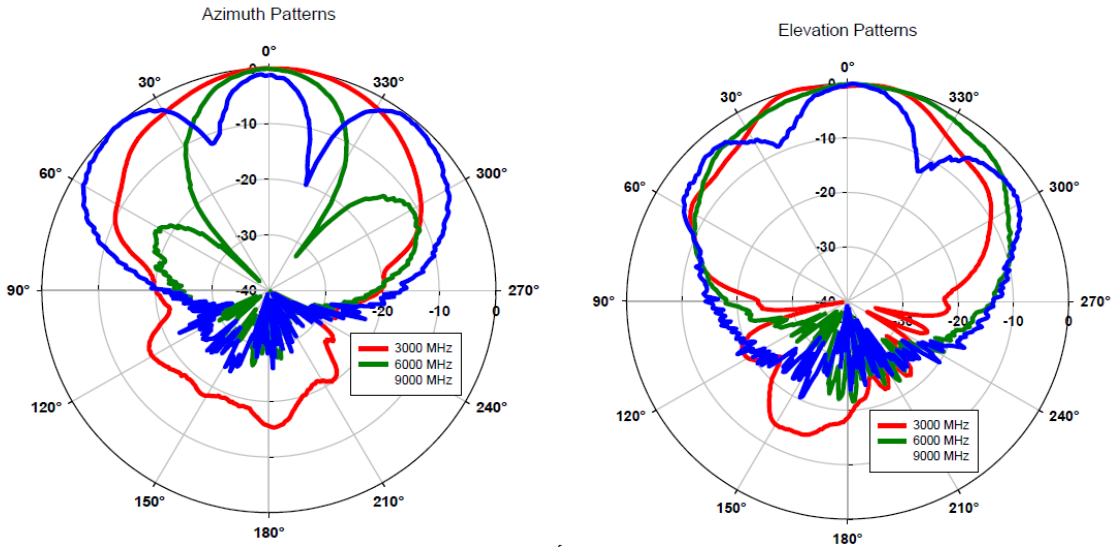


Figure 2.6 The radiation pattern for UWB antenna (Octane BW-3000-10000-EG), from left to right Azimuth and Elevation patterns of the antenna used for the UWB measurement process.

Figure 2.7 Octane BW-3000-10000-EG used for UWB Off-body channel characterization.

An IRIS+ quadcopter which is shown in the Figure 2.8 was used for the measurement, which had 6 miles of communication range, the maximum speed of 25 mph and 3 DR link communication. The python code was used for acquiring data which took approximately 10 minutes for each channel measurement.

Figure 2.8 An IRIS+ quadcopter used for placing the transmitter.

### 2.2.2. MEASUREMENT PROCEDURE

Before implementing any system design, proper planning is essential. Similarly, for the wireless system to implement, proper planning of channel measurements and modeling are indispensable [45]. It is necessary to analyze the wireless tag performance for understanding the correlation between them. We are trying to understand the difference in the behavior of UWB wireless tag in different multipath environments. In our case, we have taken measurements in three different scenarios,

- Anechoic chamber;

- Indoor (Warehouse) environment;
- Outdoor;

Before going in-depth analysis of each environment, it is important to understand each one of them fundamentally. The anechoic chamber is an environment with no reflection, whatever the signal is sent from one node to other, it is absolutely absorbed. The picture of the anechoic chamber is shown in Figure 2.9. Thick foam and Styrofoam surrounded the chamber for high absorption. Hence, such rooms are highly useful for coming up with valid conclusion on no multipath environment.

We analyzed indoor warehouse environment, which could also be considered as a practical environment. This is an environment which has a certain amount of large and small fading due to the objects around, through which the signals are reflected, and also multipath could be observed. We found there was enough scattering due to metallic scatters in the indoor warehouse environment [45]. It was considered practical, because generally in such environment a person spends most of his time. It becomes essential to study the behavior of UWB in indoor warehouse; it had unique propagation properties that consisted of substantial metallic walls, dimensions of halls and surrounding objects. Our main gain from such environment was to introduce multipath to analyze the performance of UWB wireless links.

Outdoor is an environment that is not closed or surrounded by any walls. Through this we aim to understand the UWB performance in an open space. We also tried to learn how much a wireless tag is affected by the outside environment.

For the measurement, firstly, it was important to decide a multipath environment, mostly it is advisable to take the first measurement in the anechoic chamber without any multipath. The measure is made in the frequency domain [22]. In our setup, for each scenario, a transmitter is fixed at the UAV and receiver patch is attached to a human subject. The measurement is taken for the distance range of 3.5 to 8.0 meters with the interval of 0.5 meters in the indoor warehouse.

For each distance, the antenna patch is placed at 13 different human body locations for LOS and four body locations for NLOS. The patch locations on the human body for both LOS and NLOS is shown in the Figure 2.10.

Before starting the measurement, it is essential to perform the calibration (Agilent 85032F) at the

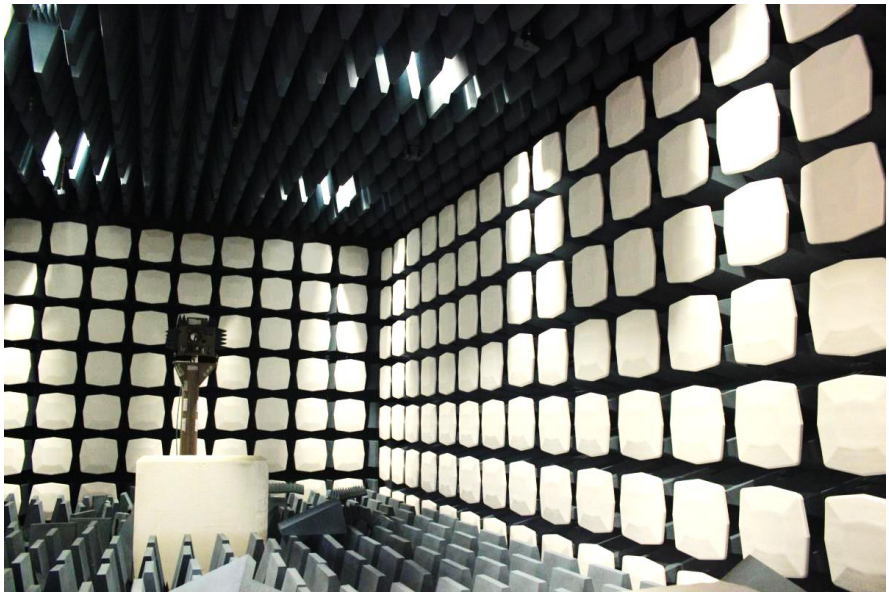

Figure 2.9 The picture of anechoic chamber where Off-body communication was performed [28].

interested frequency band for compensating the effects of measuring equipment, antennas, and cables [46], which helps in maintaining a reference to the overall system. When VNA was evaluating the channel response for each distance and each body location, it was necessary to obtain original data by extracting the effects of cables and outer environment on the final measured data.

For taking the measurement, a human subject was made to stand still, with antenna receiver patch on his body at the distance of 8 meters in the LOS with the transmitter that is attached to a UAV. All the measurements were performed in the indoor warehouse of Richmond Hill lab of Oklahoma State University, Stillwater. The layout of the lab is shown in the Figure 2.12. The walls of the warehouse were made up of steel and surrounding had two metal pillars near the measuring

environment. The plan of the indoor area in which measurements were taken along with receiver and UAV is shown in the Figure 2.11 [46]. Inside the warehouse ten different transmitter-receiver separations were selected varying from 3.5-8.0 meters with the interval of 0.5 meters. For each antenna location, two different scenarios were considered LOS and NLOS. For LOS ten, whereas for NLOS four different antenna patch locations were measured, which is shown in the Figure 2.10.

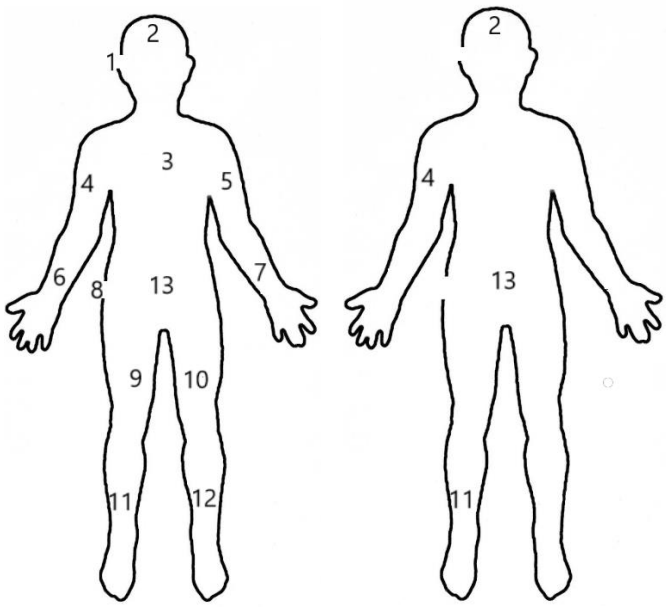


(a) (b)

Figure 2.10 The UWB antenna patch locations on human body for measurements in the (a) LOS and (b) NLOS scenarios.

For the distance of 8 meters, the UWB antenna sensor was placed at 13 different body locations, for each patch location, 10-time snapshots of measurements were collected for 1601 number of points for the uniform frequency distribution of 3.1-10.6 GHz. Then, with the interval of 0.5 meters, the subject changed his distance, and the entire measurement process was repeated every time for each of the length until human subject reached 3.5 meters. For LOS, at every interval, for each 13 body location, data, i.e., channel responses were collected. The data is nothing but frequency

response with both magnitude (dB) and phase (degrees). Throughout the measurement process, the height of transmitter (on the UAV) was maintained.

The flow chart representing the post-processing steps after the UWB channel measurement were obtained.

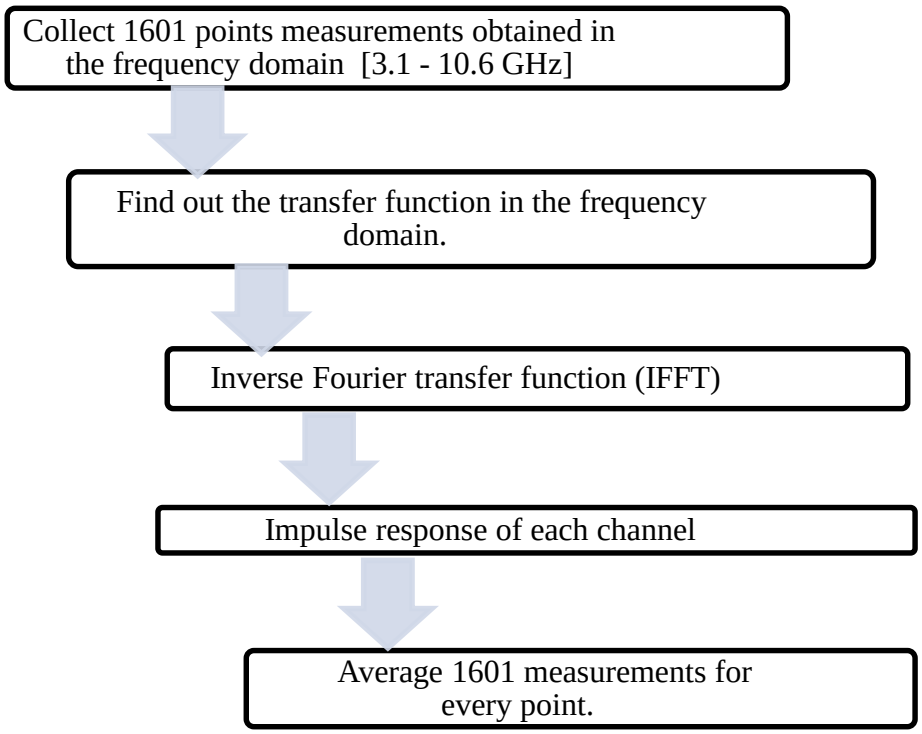


The entire measurement process was repeated for the anechoic chamber and outdoor environment. Both could be considered as extreme environments as compared with the indoor warehouse. We made sure to lock the anechoic chamber while measurements were recorded. The anechoic chamber in the Richmond Hill lab consisted of two axes, radiation absorbent material. The outdoor environment where the measurements were taken was free open but not empty, the measurement scenario had parked cars along one side. The anechoic chamber and outdoor settings are shown in the Figure 2.9 and Figure 2.13 respectively.

During the measurement, we made sure about the most basic conditions, such as no other human subject or unwanted moving objects were present in the measurement setting, to avoid Rician

fading for LOS and Rayleigh fading for NLOS scenario. For the measurement, the UAV was maintained at the fixed height of 3.0 meter. Ten sets of data was collected for different receiver location that were placed on a human subject for each new set of measurements [46]. The channel

(a) (b)

Figure 2.11 Indoor warehouse measurement setup with the human subject in the LOS with the UAV in the indoor warehouse environment with path location at (a) Ear and (b) Wrist.

response we received out of VNA was nothing but S21, i.e., also known as Transmission coefficient which corresponds to channel transfer function and kept safe for the post-processing and further evaluation of other crucial parameters.

The entire procedure was repeated for NLOS for four body locations shown in the Figure 2.10 and path loss exponent, time dispersion parameters were calculated.

While performing the measurements, it is advisable to take care of many factors. UWB propagation is heavily frequency-dependent [41]. It is suggested to have a stable static environment condition,

which means if one measurement is taken considering a bunch of people in the room then rest other measures should also be taken with the same number of people at the similar location. The objects situated on the way between transmitter and receiver in the propagation medium affects all the frequencies in different ways [41]. Studies have shown that number people in a room affect the measurement results at vast extent [22]. In our setup, we made sure that no other entity should change the measurement. Also, it is advisable to take care of the coaxial RF antenna cables and connectors, cables shouldn't be bent anywhere, and connectors should be tightened firmly to avoid the losses due to moving cables during measurement. Under these conditions, the frequency response of the channel does not vary a lot during the time required to sweep the whole measurement bandwidth [47]. Also, we took care of the distance between the body and the mounted antennas by considering 5-7 mm distance variation caused by loose clothing.

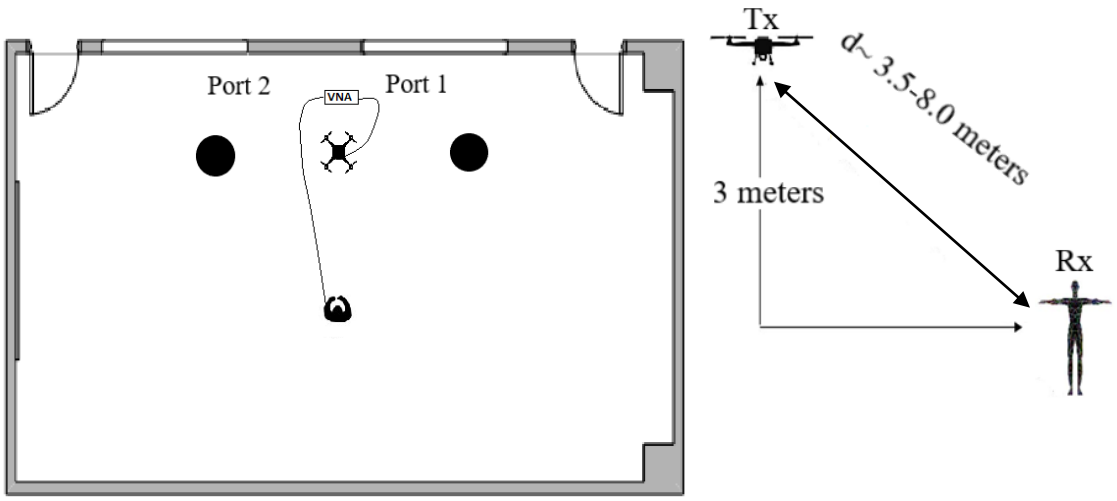


(a) (b)

Figure 2.12 (a) The layout of indoor warehouse setup, the two black spots represent two solid pillars present near the measurement setup. (b) The transmitter-receiver setup with wireless communication.

(a) (b)

Figure 2.13 Outdoor setup with human subject and in the LOS (a) side view of the setup with patch on his wrist (b) front view with patch location on his wrist.

## 2.3 PATH LOSS CHARACTERIZATION

Path loss characterization plays a vital role in designing wireless system. The primary objective of path loss characterization is to find out path loss exponent value in each environment i.e., anechoic, indoor warehouse and outdoor. The path loss exponent was supposed to be varying based on the different environment in which measurements were performed. In the practical environment, i.e., indoor and outdoor, the received power should logarithmically decrease with increasing distance. The path loss exponent also depends on antenna height and terrain category.

For our setup, the data was collected for all the distances with each body location using data acquisition device, in our case we used python code on a laptop, data was processed further for evaluating other significant parameters. The recorded values were indexed as, $H(f)$, where 1601

points were uniformly captured over the frequency range of 3.1- 10.6 GHz, which we defined as $i$ varying from 1…1601 and for each distance we took snapshots of ten readings for averaging purpose, which we defined as *j*, varying from 1…10 [47]. Before any further parameter estimation, a coherent averaging of 10 measurements over the entire frequency range of 1601 points was performed, i.e., over the ten time-snapshots for each spatial point, to reduce the noise level and increase statistical analysis reliability. UWB measurement and propagation is heavily frequency dependent that's why it was easy to model by impulse response method [41]. For mean power, time average of signal data was performed by changing position of the receiver [51]. The channel transfer function in the form of $H(f)$ for each distance is given by [47],

$$\mathrm{H}(f) = \sum_{j=1}^{10} \sum_{i=1}^{1601} S_{21}(f_{i,j})$$

By taking ten snapshots of the measurement, averaging it and integrating the output helps in compensating external and antenna effects [41]. The evaluated channel transfer functions $H(f)$ between fixed *m* transmitter and *n-th* different receiver distances which in our setup is ten, was windowed using Hamming window then inversed Fourier Transformed resulting in impulse response $h\,(\tau, m, n_i)$. When the concept of windowing is applied, we found out a measurable decrease in the number of paths counted [48]. Windowing generally improves the dynamic time domain range of a signal by neglecting the frequency response [49]. We were aiming to obtain a time domain response from a frequency domain at best, fast and easy way using Inverse Fast Fourier Transform (IFFT) method [46]. The evaluation was done for all of the ten different combinations of transmitter (Tx) and receiver (Rx) array locations, resulting in a total of 10 × 9 impulse responses [45], where 9 stands for the body positions of UWB sensor tag on a human subject which we took measurements for.

Path loss is defined as a ratio between transmitted and received power, which can be directly measured by averaging the responses obtained by measurements [50]. The path loss characterization is separately done for all the environments. In our work, the goal is to understand the variation in received signal power with distance due to path loss & shadowing. Path loss is caused to the propagation channel and the power radiated by the transmitter. Path loss in dB could be given as a linear function of the logarithmic distance between transmitter and receiver, where, the slope of the graph determines path loss exponent given as $\gamma$, which could be mathematically expressed as,

$$PL_{dB}(d) = \frac{Transmitted\ power}{Receiver\ Power} = PL_{dB}(d_o) + 10\,\gamma \log_{10}\left({}^{d}/_{d_o}\right) + X_{\sigma}$$

Where $d$ is the distance between transmitter and receiver, $d_o$ is the reference distance, and $PL(d_o)$ is the path loss at the reference distance, $\gamma$ is known as path loss exponent, $X_{\sigma}$ is a zero-mean Gaussian distributed random variable with standard deviation $\sigma$, both these values and path loss is defined in decibels (dB) [50].

The main objective behind studying the relation between path loss and distance is to calculate the value of path loss exponent for indoor and outdoor scenarios separately and compare them. As we know the value of path loss exponent is evaluated using slope, we used linear regression analysis, Least Squares method which is shown in Figure 2.17. The path loss exponent value increases with increasing number of indoor objects and also the increasing frequency, whereas, path loss exponent decreases with increasing antenna height [21]. For every distance, we averaged the obtained path loss values, which could be mathematically given as,

$$PL_{dB}(\,d_l\,) = -10\log_{10}\left(\frac{1}{1601}\sum_{i=1}^{1601}|\,H_i(d_l)|^2\,\right)$$

Where $d_l$ is each distance ranging from 3.5- 8.0 meters. The critical point here is to model the large-scale characteristics of the environment for doing that, it is indispensable to come up with path loss variation.

### 2.3.1. STATISTICAL ANALYSIS

In the radio communication system, modeling is done statistically. The statistical analysis is performed using Akaike Information Criteria (AIC) in both the indoor and outdoor environment. The cumulative distribution function (CDF) of the path loss variation in each of the scenario, i.e., indoor warehouse, and outdoor, for each body channel is compared to well-known distributions, Normal, Weibull, Lognormal, Rayleigh, Nakagami, Rician, Gamma, and Exponential which is shown in the Figure 2.14.

For the UWB statistical modeling, we try to find the best model using AIC. It is a great relative quality method for coming up with a best statistical model [23,24]. The measured data is used for coming up with different statistical models which are relatively compared by AKAIKE method.

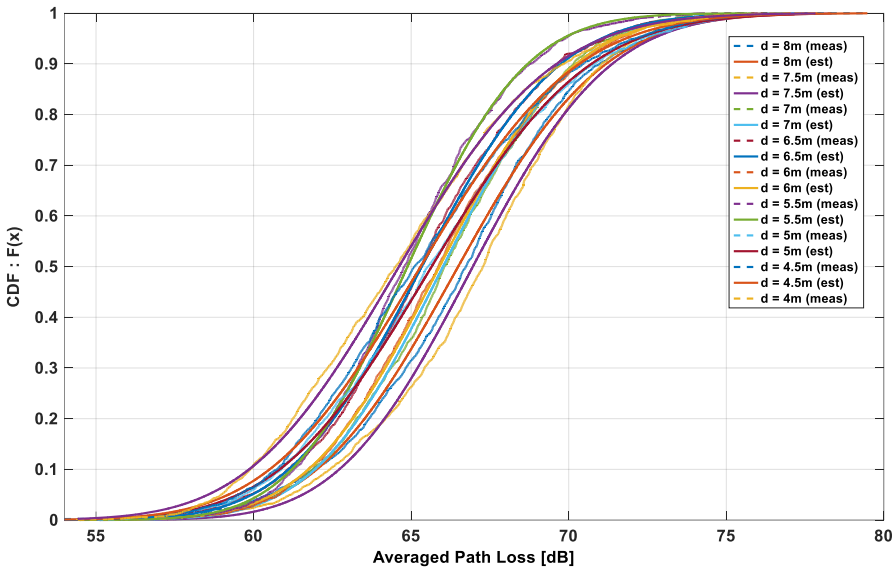


Figure 2.14 Cumulative distribution function measured and estimated, for forehead Off-body radio channel when subject was in the indoor environment at different distances.

The second order AKAI is defined as,

$$AIC_c \;=\; -2\,ln\,(L) \;+\; 2k \;+\; \frac{2k\,(k+1)}{(n-\,k-\,1)}$$

Where *L* is the maximized likelihood, *k* is the number of parameters estimated for that distribution, and *n* is the number of samples of the experiment. The eight distributions models mentioned above are all two parameter distributions *(k =2)* except the Rayleigh and the Exponential *(k = 1)* [50]. For determining the best statistical model, always look for the lowest AIC, and the idea is to sort statistical models from good to the bad ones; that's why relative AKAI is considered which normalizes to the lowest value obtained [50]. The corrected value is given by,

$$\Delta_i = AIC_C - \min\,(AIC_C).$$

If the result of any statistical model indicates zero, it represents the best fitting. In our study, we applied AKAIKE for an indoor warehouse environment. We also analyzed the best distribution pattern for the outdoor setting as well; this was evaluated to be sure about the distribution. We were curious about finding if both outdoor and indoor support the same distribution result or not, also it helped in settling up with the distribution indeed. The AIC analysis for indoor and outdoor is shown in the Table 2.1 and Table 2.2, respectively. The AIC low value shows better distribution. On the basis of the tabulated result of AIC, all the body positions we took into account for the measurement, in both indoor and outdoor environment supports Lognormal as the best fitting distribution for our system which is shown in the Figure 2.15 and 2.16. Also, the Figure 2.14 shows CDF for each distance considering Lognormal as a best distribution fit.

| Position | Normal | Weibull | Lognormal | Rayleigh | Nakagami | Rician | Gamma | Exponential |
|---|---|---|---|---|---|---|---|---|
| Forehead | 0.0036 | 42.19 | 17.27 | 4113.59 | 1.95 | 0 | 8.47 | 6292.23 |
| Heart | 3.49 | 38.6 | 4.22 | 4010.94 | 0 | 3.44 | 1.42 | 6186.814 |
| Right wrist | 15.65 | 252.95 | 0 | 5668.19 | 8.85 | 15.62 | 3.75 | 7872.35 |
| Abdomen | 0 | 19.17 | 24.12 | 4513.76 | 5.12 | 0.021 | 13.75 | 6701.5 |
| Right thigh | 41.39 | 420.11 | 0 | 5807.27 | 26.17 | 41.34 | 12.42 | 8012.53 |
| Right arm | 0.0079 | 44.176 | 10.10 | 4537.45 | 0.575 | 0 | 4.6 | 6725.8 |
| Right shin | 0 | 61.33 | 17.31 | 5166.476 | 3.71 | 0.01 | 9.75 | 7365.04 |
| Waist | 16.28 | 294.24 | 0 | 6103.48 | 9.62 | 16.26 | 4.25 | 8311.30 |
| Ear | 11.11 | 301.88 | 0 | 6380.04 | 6.31 | 11.10 | 2.59 | 8589.74 |

Table 2.2 Comparison of different distributions adopting AKAI for nine Off-body positions in the indoor environment.

| Position | Normal | Weibull | Lognormal | Rayleigh | Nakagami | Rician | Gamma | Exponential |
|---|---|---|---|---|---|---|---|---|
| Forehead | 8.42 | 64.04 | 1.25 | 3578.72 | 0.93 | 8.29 | 0 | 5740.48 |
| Heart | 94.619 | 0 | 168.10 | 3787.28 | 114.3 | 94.80 | 139.64 | 5952.79 |
| Right wrist | 27.46 | 0 | 67.61 | 5413.32 | 39.07 | 27.5 | 52.59 | 7614.53 |
| Abdomen | 12.9 | 0 | 54.57 | 4215.9 | 23.20 | 13.05 | 37.62 | 6396.71 |
| Right thigh | 23.98 | 312.98 | 0 | 5411.46 | 14.05 | 23.94 | 6.11 | 7612.86 |
| Right arm | 59.89 | 0 | 112.96 | 4130.85 | 73.77 | 59.99 | 92.17 | 6308.14 |
| Right shin | 11.05 | 204.57 | 0 | 4915.33 | 4.82 | 11.01 | 1.35 | 7110.22 |
| Waist | 12.56 | 198.90 | 0 | 5254.13 | 6.4 | 12.53 | 2.47 | 7453.75 |
| Ear | 12.361 | 189.9 | 0 | 5053.49 | 6.02 | 12. 65 | 2.20 | 7250.43 |

Table 2.3 Comparison of different distributions adopting AKAI for nine Off-body positions in the outdoor environment.

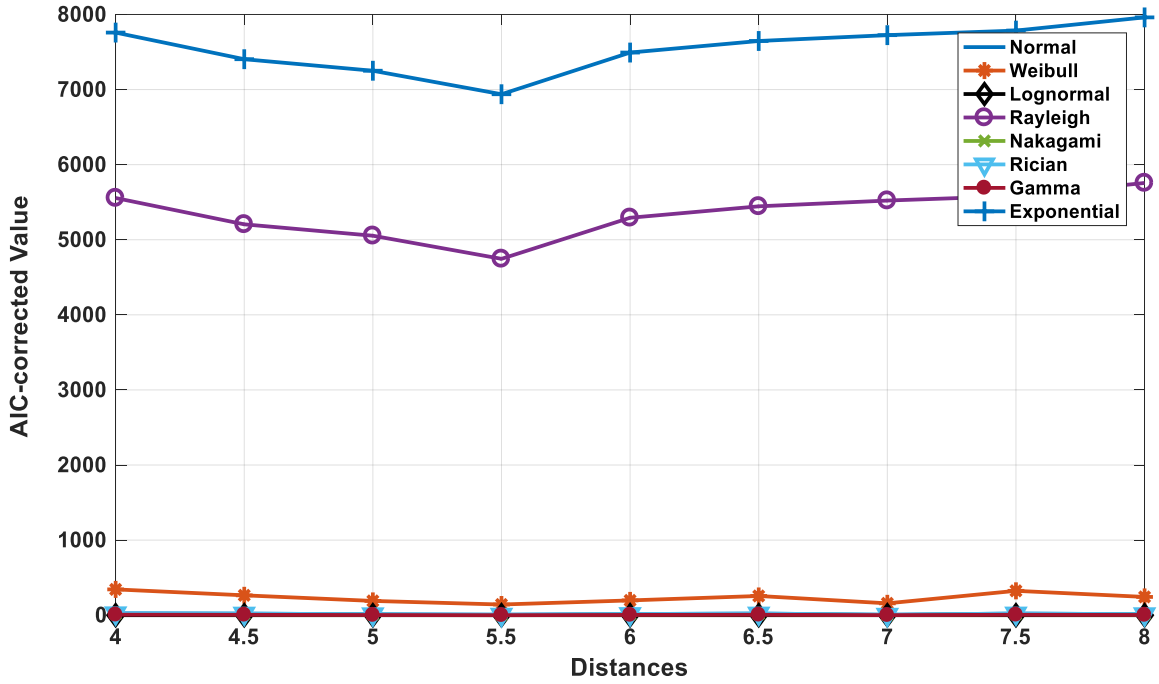


Figure 2.15 The statistical analysis representing all the distributions to fit according to AKAIKE method.

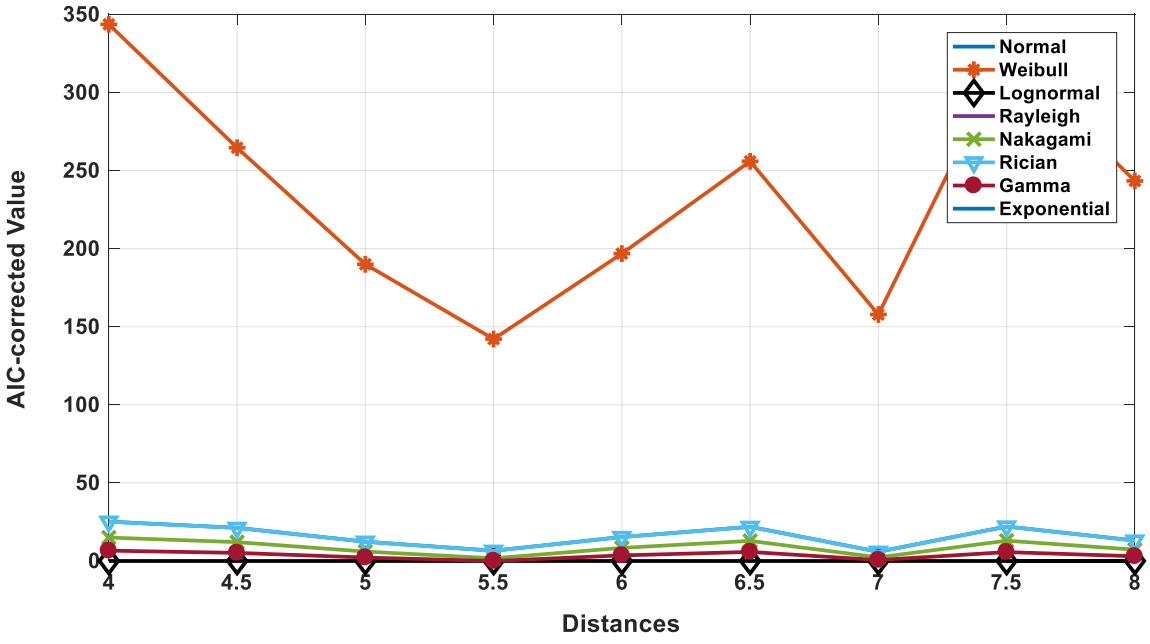


Figure 2.16 The statistical analysis representing Lognormal as a best fit out of other distributions according to AKAI method as it is close to the x-axis.

### 2.3.2. PATH LOSS ANALYSIS

Statistical analysis helped in understanding the concept behind the best suited model and further assisted in determining Lognormal as the best distribution. Once we were familiar with the distribution, the main aim of this section was to come up with the path loss exponent for each body location. Path loss exponent is a factor to categorize an environment as lossy or non-lossy. Lower the path loss exponent value represents a free space, higher the exponent value represents the lossy environment. In our experiment, the path loss exponent was compared between two situations, i.e., indoor and outdoor. While taking the measurements, we already observed and assumed, the left and right side of human body did not make much difference. Hence, considering the assumption further, we only observed human subject's right side channel path loss exponent ($\gamma$) values. Before proceeding for path loss exponent, the path loss for each body location is observed. The Table 2.4

| **Body location** | **Path loss - Indoor** | **Path loss - Outdoor** |
|---|---|---|
| Ear | 63.88 | 66.00 |
| Forehead | 59.44 | 60.10 |
| Chest | 62.14 | 60.31 |
| Right Arm | 62.64 | 63.17 |
| Right Wrist | 64.67 | 63.48 |
| Waist | 64.10 | 64.27 |
| Right Thigh | 63.89 | 63.81 |
| Right Lower Shin | 63.52 | 63.77 |
| Abdomen | 62.57 | 61.96 |
| **Overall body average** | 62.98 | 62.98 |

Table 2.4 Comparing indoor and outdoor path loss of nine body locations for LOS.

shows the path loss of individual channels in both the indoor and outdoor environments.

Through the Table 2.4 we can make two conclusions,

- The environment with high path loss overall.
- The channel with high path loss in both the environments.

After analyzing the results, we can see overall both the environment share similar path loss value of 62.9 ~ 63.0 dB. Hence, we can conclude both the environments have a similar loss. Now, if we look over and observe the individual path loss for each channel, forehead in both the environments has lower path loss. The reason behind low value is the LOS, face to face communication between transmitter and receiver. For the indoor environment, the right wrist has highest path loss of 64.67 dB, which could be because wrist movement in between the measurement due to which communication becomes NLOS. Whereas for outdoor environment, ear and waist has higher path loss of 66.00 dB and 64.27 dB. Another reason behind the differences in the value is the antenna polarization which is vertically polarized in our case, comes cross aligned with the receiver antenna for certain body positions with the transmitter antenna. Now, instead of analyzing each channel as an individual, we combined two or three body locations and considered as one single channel. For instance, the wrist and arm path loss values were averaged to call hand section. Similarly, chest section, head section, and leg section include abdomen/ waist/heart position, ear/forehead and thigh and shin, respectively.

The Table 2.5 shows all the combined results of path losses.

| Combined body channels | Indoor | Outdoor |
|---|---|---|
| Head | 61.66 | 63.05 |
| Chest | 62.9 | 62.2 |
| Hand | 63.65 | 63.33 |
| Leg | 63.70 | 63.79 |

Table 2.5 Comparing indoor and outdoor path loss value of four combined body channels for LOS.

On the combined analysis of path loss for four sections, we observed leg had higher path loss value for both indoor and outdoor environments. Leg led all other sections by the value of 63.7 and 63.79 for both indoor and outdoor, respectively. The reason behind is that the higher value has to cover

more distance between the transmitter and receiver for wireless communication. Also, antenna suffered from ground reflections and gave rise to the high loss.

In each environment, indoor and outdoor, first the path loss pattern was studied for LOS, we took measurements for nine body locations, which included only the right side of the human subject i.e., right ear / arm / wrist / thigh / lower shin, forehead, chest, waist and abdomen, as per the prior assumption of symmetry. Moreover, the path loss exponent in LOS is observed for nine body locations. The comparison of path loss exponent is shown in the Table 2.6.

| **Body location** | **Path loss exponent - Indoor** | **Path loss exponent - Outdoor** |
|---|---|---|
| Ear | 0.31 | 0.57 |
| Forehead | 1.80 | 1.22 |
| Chest | 0.19 | 1.05 |
| Right Arm | 0.05 | 0.94 |
| Right wrist | 0.34 | 0.32 |
| Waist | 0.96 | 0.85 |
| Right Thigh | 0.21 | 0.58 |
| Right Lower Shin | 0.26 | 0.13 |
| Abdomen | 0.51 | 0.58 |
| **Overall body average** | 0.51 | 0.69 |

Table 2.6 Comparing indoor and outdoor path loss exponent value of nine body locations for LOS.

From Table 2.6 we observed, outdoor has higher path loss exponent value for overall body as compared to indoor. Outdoor overall exponent leads by the value of 0.69. For both indoor and outdoor, the higher value of path loss exponent was obtained for the forehead, i.e., 1.8 and 1.22, respectively. However, for both indoor and outdoor environment path loss exponent has high value for forehead location, the reason is, communication is less distant between the transmitter and receiver because forehead area is closer to the UAV as compared to any other body section

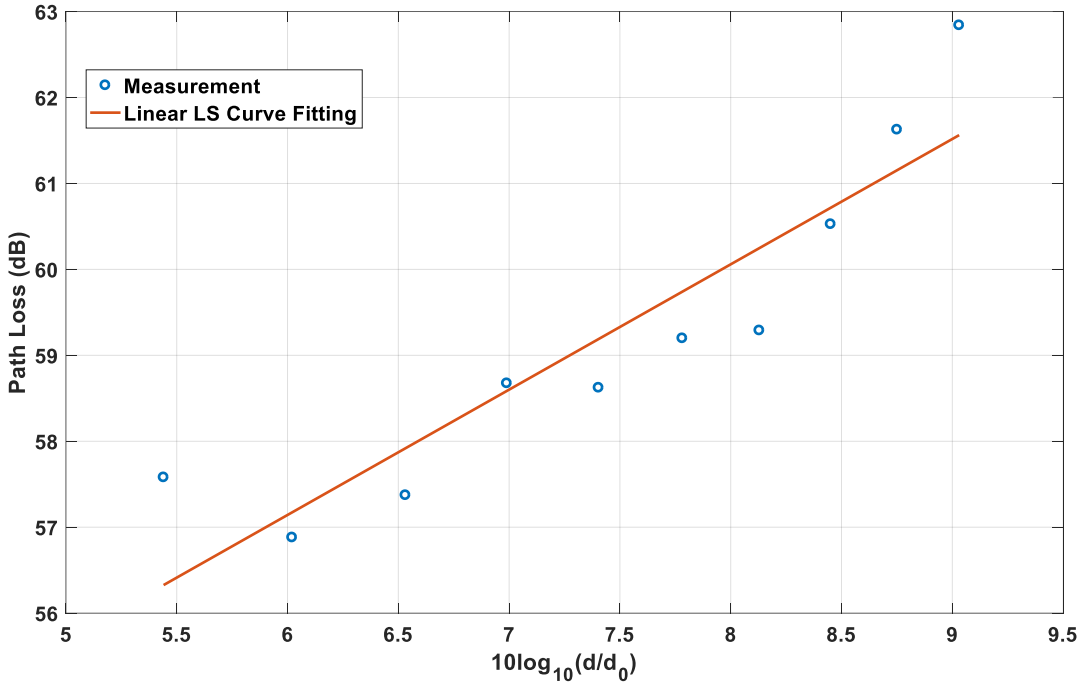


Figure 2.17 For forehead and waist combined in the indoor environment, estimating slope i.e., finding path loss exponent using linear regression, Least Squares method.

and hence in proper polarization with each other. For indoor, right arm has low path loss exponent value of 0.05, whereas, for outdoor, lower shin has low exponent value 0.13. The probable reason behind the low values for path loss exponent in both the environment would be multipath effect due to surrounding objects. Also, we observed the path loss exponent value by combining the effects of body location as an overall channel. Instead of comparing individual body location, the averaged path loss exponent value of indoor and outdoor is shown in the Table 2.7.

| Combined body channels | Indoor | Outdoor |
|---|---|---|
| Head | 1.05 | 0.89 |
| Chest | 0.55 | 0.82 |
| Hand | 0.19 | 0.63 |
| Leg | 0.24 | 0.36 |

Table 2.7 Comparing indoor and outdoor path loss exponent of four combined body channels for LOS.

In the combined analysis of body channels, for both indoor and outdoor the path loss exponent value is higher for head section, i.e., 1.05 and 0.89. In indoor, the lower value of path loss exponent is observed for hand section, whereas, for the outdoor leg has low path loss exponent value, as 0.19 and 0.36 respectively.

After analyzing the LOS, we observed the same pattern for NLOS in both the environments. As we did not take measurements for all the body locations in case of non-line of sight, we observe four body locations only, i.e., forehead, right arm, right lower shin, and abdomen because human subject was not facing the antenna patch attached to the UAV; hence, we picked body location from each section of the human body. The path loss value for each position in NLOS scenario for both the environments is given in the Table 2.8.

| Body patch location | Indoor | Outdoor |
|---|---|---|
| Forehead | 66.98 | 66.44 |
| Right Arm | 69.20 | 68.63 |
| Right Lower Shin | 68.97 | 69.32 |
| Abdomen | 69.32 | 67.60 |

Table 2.8 Path loss values for both the environments of each body section in NLOS.

For NLOS, in both the indoor and outdoor environments, forehead has a low value of path loss. Whereas for the higher value of path loss both the environment has a different value of body locations, for indoor environment, abdomen has a high loss, whereas, in outdoor lower shin has the higher value.

To understand the environments in which the human subject was exposed the path loss exponent was determined for NLOS environment as well which is shown in the Table 2.9. By covering the NLOS we are planning to analyze the shadowing scenario which is one of the studies to be performed to understand the large scale fading.

| Body patch location | Indoor | Outdoor |
|---|---|---|
| Forehead | 1.12 | 0.61 |
| Right Arm | 0.26 | 0.38 |
| Right Lower Shin | 0.03 | 0.15 |
| Abdomen | 0.11 | 0.50 |

Table 2.9 Comparing indoor and outdoor path loss exponent value of four body locations for NLOS.

As we can see from the Table 2.9, the higher value of path loss exponent is observed for forehead in both indoor and outdoor environments as 1.12 and 0.61 respectively. The minimum exponent is observed for lower shin in both indoor and outdoor environments.

Hence, for both LOS and NLOS we can infer that forehead is the best location for a sensor, which makes sense because more it would be closer and in the LOS to the UAV. We also observed when sensors are not aligned properly and disrupts the communication; it gives rise to overall path loss.

## 2.4 TIME DISPERSION PARAMETER

Time dispersion parameters are the perfect way to find out the delay in the system. The multipath in the channel creates time delay spread that is a characteristics of the channel, which leads to, time-varying channel [39]. In this section, we study about the power delay profile, RMS delay, mean and max excess delay. The time spreading could be explained as [39],

$1/t < (f2 - f1)$, leads to little time spreading.

$1/t > (f2 - f1)$, leads to enough time spreading & distortion.

For delay analysis, the frequency responses or channel transfer functions we obtained after measurement were averaged, then the impulse response is received for each body channel, which could further lead to parameters calculation. The acquired impulse response goes through Hamming

windowing [35] and normalization. Windowing improves in the dynamic range of the time domain transform of data and produces an impulse stimulus with lower side-lobes but broader pulse width [43]. After windowing, IFFT was applied that transformed frequency domain to time domain.

It is impossible to obtain the time parameters without calculating the power delay profile(PDP). Also, it is impossible to find PDP without finding the impulse response. Power delay profile could be calculated as [43],

$$P\,(\tau, d_l)\;=\;|h\,(\tau, d_l)|^2$$

Where $\tau$ represents the delay for some distance $d_l$, $h\,(\tau, d_l)$ is the Fourier transform of $S_{21}$ in the frequency domain.

We calculated one of the the time dispersion parameters, i.e. Max excess delay for a set threshold value of 5 dB; also, we have the flexibility of changing the threshold value to as per our requirement. We derive other multipath dispersion parameters mathematically from power delay profile, which is represented by relative received power and excess delay with respect to fixed time.

The mean excess delay is the first moment of power delay profile and is given as [43],

$$\tau_m\;=\;\frac{\sum_i P(\tau_i)\tau_i}{\sum_i P(\tau_i)}$$

The RMS or root mean square delay spread is one crucial time dispersion parameter. More importantly, when frequency bandwidth is too high, RMS delay is must to be studied. It provides a measure of time dispersion in multipath and evaluates the performance of the system [46]. UWB has a massive bandwidth of 7.5 GHz due to which it doesn't support flat fading hence frequency selective fading is prominent, that's why RMS delay spread plays an important role. Mathematically, it is given as the square root of the second moment of power delay profile [43],

$$\tau_{\text{rms}} = \sqrt{\tau^2 - {\tau_m}^2}, \quad \tau^2 = \frac{\sum_i P(\tau_i)(\tau_i^2)}{\sum_i P(\tau_i)}$$

Maximum excess delay of the power delay profile could be determined by the time delay during which multipath energy falls to the set threshold value (In our setup 5 dB).

After understanding the delay parameters, the implementation of delay analysis in our experimental setup we are observing each body location separately, and it is essential to note the pattern of delay for each one of them in both the scenarios indoor and outdoor. Also, for an ideal environment consideration, we measured the anechoic chamber, and the pattern of average delay profile for the anechoic chamber is shown in Figure 2.18.

As we observed in the path loss characterization, for both LOS and NLOS scenario, we determined the path loss and path loss exponent for each body location in both the environment indoor and outdoor.

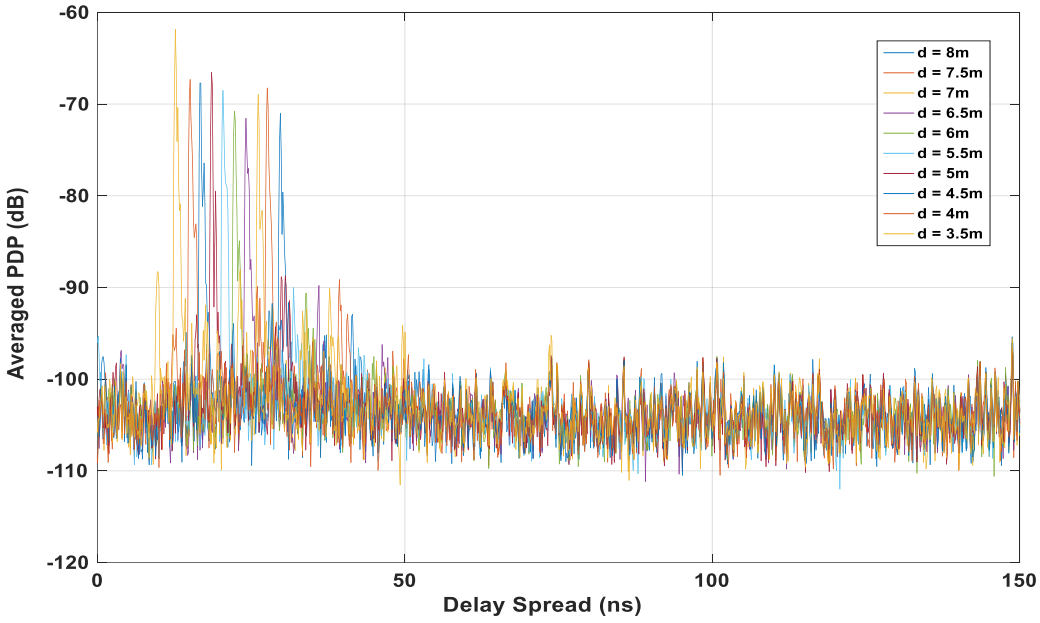


Figure 2.18 Average Power delay profile for each distance (*d*) in the anechoic chamber environment.

The pattern followed by body channels in determining the path loss helped in understanding the origin behind it, also, helped in finding out the best sensor location in both LOS and NLOS.

| Body patch location | RMS delay- Indoor (ns) | RMS delay-Outdoor (ns) |
|---|---|---|
| Ear | 43.3 | 64.2 |
| Forehead | 30.5 | 64.0 |
| Chest | 42.9 | 41.6 |
| Right Arm | 46.0 | 60.7 |
| Right wrist | 56.8 | 61.2 |
| Waist | 48.6 | 59.2 |
| Right Thigh | 49.6 | 55.1 |
| Right Lower Shin | 48.2 | 51.5 |
| Abdomen | 40.9 | 58.3 |
| **Overall body average** | 45.2 | 57.3 |

Table 2.10 Comparing indoor and outdoor RMS delay value of nine body locations for LOS.

Now, a similar observation made about the delay for each body location. The RMS delay pattern was observed for each sensor location. As we discussed, RMS delay is one important delay analysis for such colossal bandwidth of communication system. By finding RMS delay value for each body location, we gained a better picture of which position of the sensor makes more sense.

The RMS delay analysis is shown in the Table 2.10. The RMS delay pattern shows; the delay is higher for the outdoor environment as compared to indoor. The RMS delay has a value of 57.3 ns, whereas, for indoor, it is 45.2 ns. If we analyze the individual body location for indoor, we found out wrist has the highest delay of 56.8 ns which is high compared to the overall average for the body. The reason behind such hike for wrist could be due to the subject's small hand movements, also due to multipath from around the objects. It was good to see how little change in body position and movement give rise to such enormous delays. In the outdoor environment, the highest delay was observed for ear 64.2 ns, the only reason behind this delay is multipath between transmitter and receiver while communication was taking place.

Similarly, NLOS scenario is analyzed for the RMS delay in both indoor and outdoor, the results of the analysis are shown in the Table 2.11.

| Body channels | RMS delay- Indoor (ns) | RMS delay- Outdoor(ns) |
|---|---|---|
| Forehead | 61.0 | 64.0 |
| Right Arm | 58.9 | 62.0 |
| Right Lower Shin | 58.9 | 62.5 |
| Abdomen | 57.3 | 61.4 |
| **Overall body average** | 59.0 | 62.4 |

Table 2.11 Comparing indoor and outdoor RMS delay value of four body locations for NLOS.

We can observe from the Table 2.11, in both indoor and outdoor environment, forehead has the highest RMS delay value of 61 ns and 64 ns respectively, whereas, the least delay is observed for the abdomen. As we saw in the Table 2.10 for the indoor, forehead has lowest average RMS delay value of 30.5 ns, which is lowest as compared to any RMS delay, we have seen so far. Therefore, this forehead position was analyzed for observing other delay patterns such as the maximum excess delay and mean excess delay was also examined graphically. The spread plot for all the delays is shown in the Figure 2.19. Based upon the figure, the average of max excess delay is 20.7 ns and the average of mean excess delay is 29.3 ns.

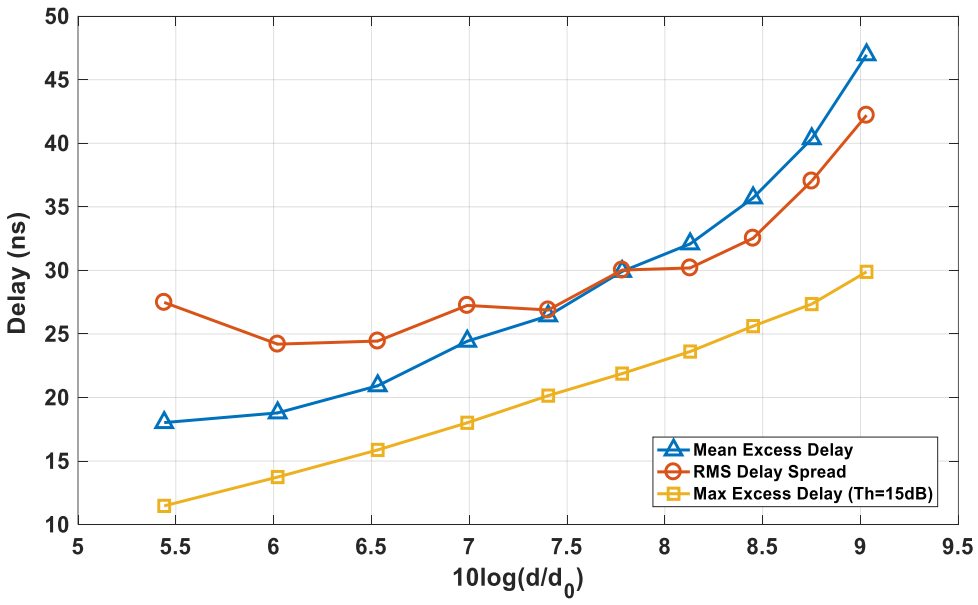


Figure 2.19 The delay pattern when antenna patch is at the Forehead position in the indoor environment (LOS).

| Body patch location | Mean excess delay- Indoor (ns) | Mean excess delay- Outdoor (ns) |
|---|---|---|
| Ear | 40.0 | 86.6 |
| Forehead | 30 | 49.8 |
| Chest | 40.08 | 37.6 |
| Right Arm | 43.1 | 66.5 |
| Right wrist | 62.1 | 67 |
| Waist | 47.2 | 63.7 |
| Right Thigh | 48.5 | 54.2 |
| Right Lower Shin | 49.2 | 50.2 |
| Abdomen | 38.4 | 59.2 |
| **Overall body average** | 44.2 | 59.4 |

Table 2.12 Comparing indoor and outdoor mean excess delay value of nine body locations for LOS.

| Body patch location | Mean delay- Indoor (ns) | Mean delay-Outdoor(ns) |
|---|---|---|
| Forehead | 81.9 | 92.3 |
| Right Arm | 107 | 106 |
| Right Lower Shin | 110 | 103 |
| Abdomen | 110.8 | 106 |
| **Overall body average** | 102.4 | 101.8 |

Table 2.13 Comparing indoor and outdoor mean excess delay value of four body locations for NLOS.

| Body patch location | Max excess delay- Indoor (ns) | Max excess delay- Outdoor (ns) |
|---|---|---|
| Ear | 22 | 13.6 |
| Forehead | 21.7 | 22.6 |
| Chest | 22.5 | 22.6 |
| Right Arm | 23.1 | 12.7 |
| Right wrist | 73.5 | 16 |
| Waist | 41 | 12.7 |
| Right Thigh | 24.5 | 25 |
| Right Lower Shin | 40.2 | 24.9 |
| Abdomen | 22.6 | 68.4 |
| **Overall body average** | 32.34 | 24.2 |

Table 2.14 Comparing indoor and outdoor max excess delay value of nine body locations for LOS.

| Body patch location | Max excess Delay-Indoor (ns) | Max excess Delay-Outdoor (ns) |
|---|---|---|
| Forehead | 135 | 152 |
| Right Arm | 213 | 213 |
| Right Lower Shin | 213 | 213 |
| Abdomen | 209 | 213 |
| **Overall body average** | 192.5 | 197.7 |

Table 2.15 Comparing indoor and outdoor max excess delay value of four body locations for NLOS.

Similarly, the mean and max excess delay is analyzed for each body location in both the environments indoor and outdoor which is shown in the Tables 2.12, 2.13, 2.14 and 2.15.

## 2.5. CONCLUSION

In this chapter, we started with explaining the significance of UWB communication and its importance in the wireless world. We talked about one of the crucial applications of UWB, i.e., body-centric communication. The two different kinds of body-centric communication were explained. As we were interested in Off body channel characterization, so the measurement technique which was one of the significant steps for the characterization, was covered. Entire measurement process was explained, measurement setup details were covered for both LOS and NLOS. Statistical analysis was performed for finding out the best distribution using AIC test. Path loss characterization for each body location was evaluated and tabulated. Through path loss characterization we refer, both path loss and path loss exponent value. After the path loss analysis based on their results, the delay analysis was performed for finding out more about each body location. Also, RMS delay value, max excess and mean excess delay for each body location was observed and tabulated for both LOS and NLOS.

CHAPTER III

# OFF-BODY CHANNEL CHARACTERIZATION FOR DIFFERENT POSTURES

## 3.1 INTRODUCTION

In Chapter 2, we understood the fundamentals of UWB communication and also covered one of the essential applications, i.e., body-centric communication, in the form of Off-body communication. The Off-body channel was studied, analyzed and characterized thoroughly for both indoor and outdoor measurement scenarios. The path loss and path loss exponent were determined for each body position. Also, the delay analysis was performed and based upon the analysis of path loss characterization.

In this chapter, we are extending our study to analyze different human body postures. In this study, we want to understand how UWB Off-body channel characterization is affected when the human subject stands in different postures. This study is important because understanding the LOS and NLOS behavior of each channel is not enough. By considering the postures, we are trying to consider a human subject in a practical scenario, performing quotidian activities. Before proceeding any further, it is important to decide the environment in which measurements would be taken. Previously, we wanted to study indoor environment for posture study but later on, to have a comparable environment we considered outdoor setting as well and practiced the entire measurement process with two body locations and four body postures.

In this study we did not consider all body positions; instead, we decided to go for two body positions only, i.e., forehead and abdomen, for each posture in both the measuring environments, i.e., indoor and outdoor. In addition, we have taken all our measurements in LOS scenario, i.e., human subject facing the UAV.

The primary objective of this chapter is to study the path loss variation for each of the location on the human body with different postures. This study is going to help in analyzing which posture contributes more path loss. The delay analysis for each posture would be studied as well. In the next section we have explained the entire measurement procedure.

## 3.2 MEASUREMENT METHODOLOGY

The process of measurement is similar to what we have discussed earlier, in Chapter 2. As we were performing the Off-body channel characterization, we needed the same setup and equipment. For the equipment and their specifications refer Table 2.1 from Chapter 2.

A VNA was provided same input as performed earlier. Before starting the measurement process, the calibration of the system was performed using short, open and load connectors. The external effect of cables was eradicated using Thru connector. After completing the calibration, the output is checked over the Smith plot in the VNA, for being sure regarding the calibration.

Unlike the previous measurement, where the human subject was changing his distance ranging from 3.5 – 8 meters with the interval of 0.5 meters, in this measurement setup, the human subject was standing at the fixed distance of 6 meters. Both transmitter and receiver were at a fixed distance in this measurement scenario. The measurement was performed in both the indoor and outdoor environments. Four primary postures were picked for performing the measurement, sitting, standing, bending and sleeping as shown in the Figure 3.1. For each pose, the antenna patch was

attached at two different positions on the human subject, i.e., forehead and abdomen as shown in Figure 3.2.

For the first measurement, in the indoor environment, the subject was standing with the antenna patch attached to his forehead as shown in Figure 3.3. Then subject changes the location of the antenna to the abdomen. For the second measurement, the subject is bending with the antenna attached to his forehead and later to his abdomen. Similarly, the measurement was taken for sleeping and sitting postures as well. The entire process is repeated for outdoor environment which is shown in the Figure 3.4.

(a) (b) (c) (d)

Figure 3.1 The four selected human body postures (a) Standing (b) Sleeping (c) Sitting (d) Bending.

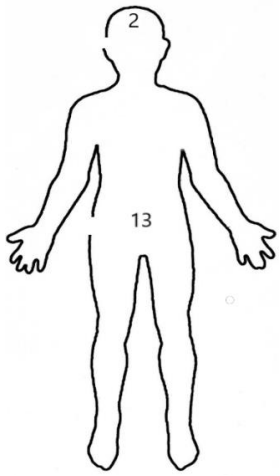


Figure 3.2 The UWB antenna patch locations on human body for measurement.

Figure 3.3 A standing human subject with UWB antenna patch attached to his forehead with the transmitter to the UAV in the indoor warehouse environment.

Figure 3.4 A standing human subject with UWB antenna patch attached to his forehead with the transmitter to the UAV in the outdoor environment.

While taking the measurement, we made sure cables were tightly held via connectors. Addition, the cables were not bent anywhere while laying on the ground. No other moving object or individual except the human subject was around the experimental area when VNA was recording the data. We made sure to secure the height of the UAV as at 3 meters.

## 3.3 PATH LOSS CHARACTERIZATION

We already discussed about studying the importance of finding out path loss, it plays a necessary role in designing any system. Path loss is like air which exists, affects us and whose presence cannot be denied at all. Path loss could not be eradicated from the system, it could only be reduced in certain ways. When we discuss about path loss characterization we refer to the path loss in the system which could arise due to many factors like diffraction, reflection or scattering by the objects in the environment. It is difficult to maintain an ideal environment for the propagation of the signal, in any experiment ideal environment would just be considered for the reference purpose, in our experimental setup, we considered anechoic chamber as an ideal environment. However, to study the practical world it is crucial to have analyzed results from both indoor and outdoor environment, it helps in understanding the path loss in easier and empirical manner.

In the previous chapter, we already studied path loss exponent in both indoor and outdoor environments. In this chapter, we want to find out the path loss values for different postures and understand the cause behind its nature, based upon the results we want to conclude which posture and body location combination suits the best. For coming up with path loss values, at first, the data, i.e., frequency response or channel transfer function ($S_{21}$) is obtained via VNA is shown in the Figure 3.5.

The data is processed through the system for converting frequency domain to time domain, that is what the entire concept on which UWB works. For the conversion from one domain to other, we use a fast and easy method of IFFT. Hence, the path loss is obtained after processing the data through the MATLAB code. The results of path loss is shown in the Table 3.1.

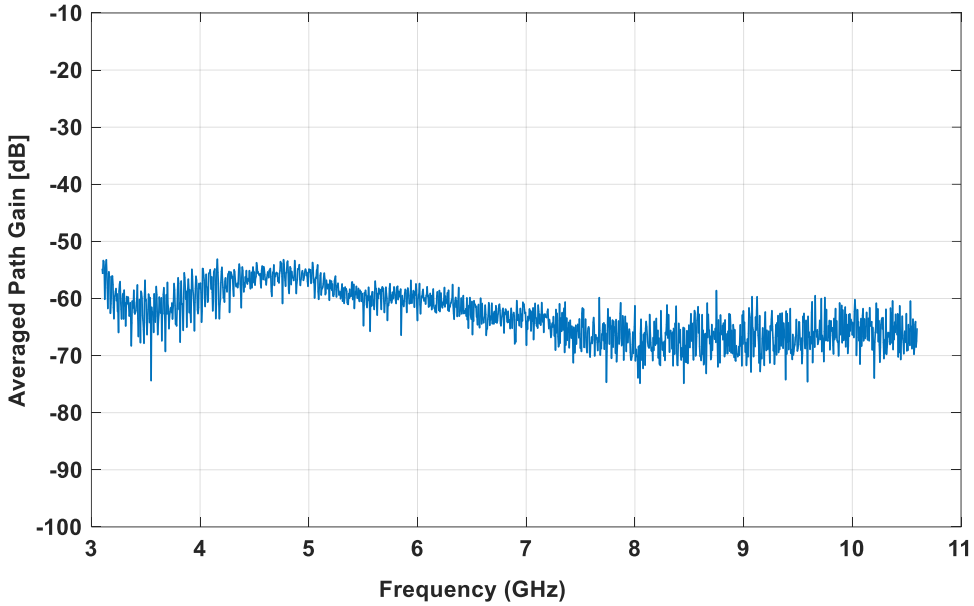


Figure 3.5 The averaged path gain vs frequency range of 3.1- 10.6 GHz for all ten points measured when antenna patch was placed at the forehead of the human subject.

| Tag location | Stand (dB) | Bend (dB) | Sit (dB) | Sleep (dB) |
|---|---|---|---|---|
| Forehead | 59.198 | 67.024 | 60.604 | 67.844 |
| Abdomen | 62.336 | 65.127 | 63.335 | 66.828 |

Table 3.1 Path loss values for two body locations and four different body postures in the indoor environment.

| Tag location | Stand (dB) | Bend (dB) | Sit (dB) | Sleep (dB) |
|---|---|---|---|---|
| Forehead | 59.63 | 68.30 | 62.38 | 68.97 |
| Abdomen | 61.48 | 68.46 | 60.31 | 67.53 |

Table 3.2 Path loss values for two body locations and four different body postures in the outdoor environment.

Through Tables 3.1 and 3.2, we can observe, stand and sit have lower path loss value as compared to bend and sleep for both the UWB based sensor locations. The one major reason behind the lower path loss value is unobstructed communication between transmitter and receiver due to LOS. We already suspected such behavior, but it was good to see the results. The best combination of posture

and position is when the person was standing with sensor tag on the forehead or sitting with the sensor on the forehead.

## 3.4 TIME DISPERSION PARAMETER

Time dispersion parameters are nothing but to understand the delay in the system; it is probable to see the delay profile following the same pattern as path loss. The posture and body location with high path loss should have a high RMS delay as well. The power delay profile, mean excess, maximum excess and RMS delay profile for four body posture with two positions of sensor locations were studied, analyzed and conclusions were drawn.

| Tag location | Stand (ns) | Bend (ns) | Sit (ns) | Sleep (ns) |
|---|---|---|---|---|
| Forehead | 30.02 | 61.45 | 34.46 | 61.19 |
| Abdomen | 38.78 | 56.36 | 39.00 | 61.76 |

Table 3.3 RMS delay for all the eight posture-sensor location combinations in the indoor environment.

| Tag location | Stand (ns) | Bend (ns) | Sit (ns) | Sleep (ns) |
|---|---|---|---|---|
| Forehead | 50.14 | 63.03 | 56.40 | 64.94 |
| Abdomen | 57.48 | 63.86 | 35.81 | 61.95 |

Table 3.4 RMS delay for all the eight posture-sensor location combinations in the outdoor environment.

From the Table 3.3 and Table 3.4, we can conclude overall RMS delay for standing and sitting is small as compared to bending and sleeping postures in both indoor and outdoor. Among all the posture and sensor position combination, a person standing with sensor on the forehead is one best combination, due to least RMS delay value.

| Tag location | Stand (ns) | Bend (ns) | Sit (ns) | Sleep (ns) |
|---|---|---|---|---|
| Forehead | 21.75 | 24.84 | 22.5 | 23.35 |
| Abdomen | 22.28 | 22.68 | 23.08 | 23.08 |

Table 3.5 Maximum excess delay for all eight posture-sensor location combinations for 5 dB of threshold in the indoor environment.

| Tag location | Stand (ns) | Bend (ns) | Sit (ns) | Sleep (ns) |
|---|---|---|---|---|
| Forehead | 22.28 | 24.68 | 22.81 | 24.68 |
| Abdomen | 22.94 | 26.01 | 23.88 | 23.88 |

Table 3.6 Maximum excess delay for all eight posture-sensor location combinations for 5 dB of threshold in the outdoor environment.

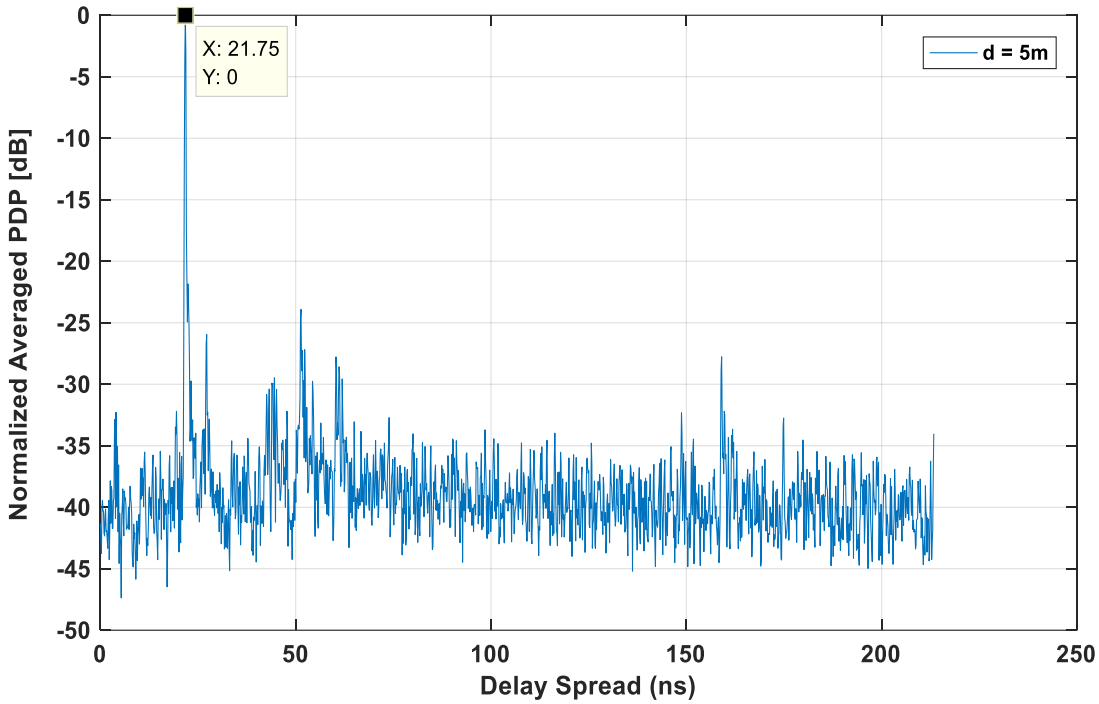


Figure 3.6 The peak in the graph between power delay profile and delay spread represents the max excess delay value of 21.75 for the sensor location of forehead while the subject was standing at the distance of 5 meters.

From the Table 3.5 and Table 3.6, we can conclude overall maximum excess delay is small and somewhat similar for all the postures in both indoor and outdoor. Among all the posture and sensor

| Tag location | Stand (ns) | Bend (ns) | Sit (ns) | Sleep (ns) |
|---|---|---|---|---|
| Forehead | 29.92 | 70.47 | 33.53 | 73.30 |
| Abdomen | 36.34 | 58.57 | 37.10 | 75.16 |

Table 3.7 Mean excess delay for all eight posture and sensor location combinations in the indoor environment.

position combination, a person standing with sensor on the forehead is one best combination and has least maximum excess delay value for the threshold value of 5 dB.

| Tag location | Stand (ns) | Bend (ns) | Sit (ns) | Sleep (ns) |
|---|---|---|---|---|
| Forehead | 45.81 | 103.00 | 55.9 | 92.01 |
| Abdomen | 57.60 | 94.78 | 34.79 | 70.73 |

Table 3.8 Mean excess delay for all eight posture and sensor location combinations in the outdoor environment.

From the Tables 3.7 and 3.8, we can conclude overall mean excess delay is small for standing and sitting posture as compared to sleeping and bending postures in both indoor and outdoor. It is due to LOS and NLOS between the transmitter and the receiver antenna, also, the antenna polarization between transmitter and receiver affects the bending and the sleeping postures. Among all the posture and sensor position combination, a person standing with sensor on the forehead is one best combination, due to least mean excess delay value.

## 3.5 CONCLUSION

In this chapter, we tried to understand the behavior of UWB sensor for different postures. In Chapter 2, we talked about how each location of the sensor on human body gets affected by different environment. We thoroughly studied about path loss and its exponents in indoor and outdoor environments, after path loss analysis we focused on the delay analysis for overall atmosphere and each sensor location. In this Chapter we followed the same pattern; first, we picked the best common postures, with each pose we picked two sensor locations, forehead, and abdomen. We analyzed path loss for the combination of sensor locations and poses, and figured out the best combination based on the tabulated results. After examining path loss, we tried understanding the delay profile for each combination, which further helped in making a stringent decision regarding the best sensor location. Also, improved in understanding the cause of each posture-sensor combination. We also realized how signals show suspicious behavior in LOS and NLOS in both indoor and outdoor environments.

# CHAPTER IV

# FINAL CONCLUSION

## 4.1 INTRODUCTION

This work presents results obtained from an Off-body UWB communication measurements at Richmond Hill lab, Oklahoma State University. In this work, we started with discussing the UWB concepts and its importance. One of the significant applications of UWB is body-centric communication; we covered one type of body-centric communication in our work. So far, many researchers have worked on the On-body communication system. On-body is a system in which both transmitter and receiver are on the human subject. In our study, we worked on the characterization of Off-body communication in which transmitter was attached to the UAV and receiver to the human subject.

We started with deciding upon the UWB sensor locations on the human body, then the distance range for which we wanted to take measurements. The primary objective of the Off-body characterization was to analyze the path loss pattern with increasing distances. Additionally, we were interested in understanding how the path loss was varying based on the sensor location on the human subject. During path loss characterization, we explored a wide range of path loss exponent ($\gamma$) value and observed for some cases it was well below 2 and in most cases below 1. The main reason behind the behavior for such wide range of path loss exponent is the multipath indoor and outdoor environment. We studied the path loss and delay variations related to them.

We observed with increasing distances between transmitter and receiver the path loss increases as well, as UWB signals were covering more distances and due to multipath in the propagation medium, the signal strength reduced giving rise to the path loss. The importance of multipath in both LOS and NLOS scenarios were observed.

While analyzing the delay we defined the threshold value as 5 dB, the threshold value applied at the PDP limited the maximum excess delay, which helped in finding out the maximum excess delay value for each body position. While analyzing the RMS delay values we observed it followed the pattern of path loss, a signal with high path loss encountered more delay.

In this work, we have also shown the statistical analysis for picking one best distribution, we used AIC method for comparing all eight different distributions, i.e., Normal, Weibull, Lognormal, Rayleigh, Nakagami, Rician, Gamma, and Exponential. We found out AIC value for all the distributions for each measured body position, i.e., forehead, chest, ear, wrist, arm, thigh, shin, abdomen. On comparing the AIC value, we found out Lognormal fits as the best distribution for our UWB system. Later, the path loss calculations; time dispersion parameters were evaluated considering lognormal distribution.

After the analysis, we found out the forehead came out to be the best position for attaching the sensor. The path loss value for forehead was less compared to other locations. Moreover, all the delay parameters came out be very low for forehead and chest. In Chapter 3, we picked four postures sitting, standing, bending, sleeping and found out sitting and standing were comparably better ones, with low path loss and delay values. The best posture-sensor location combination we found out was human sitting or standing with the sensor on his forehead. We could conclude about it by observing the path loss value and comparing it with other posture-sensor combinations, the path loss value for the standing-forehead combination was 59 dB. Also, the delay analysis provided 30 ns of RMS delay, 21 ns of max excess delay and 29 ns of mean excess delay.

## 4.2 FUTURE WORK

UWB is a growing area of research, the reason is it is not limited to one application, instead it has application in wide area from data transfer to positioning, it is more like a sea of possibilities. As we know that UWB could be used for high data transfer, one future work for this application is possibility to process and transmit a large amount of data and transfer vital information using UWB wireless body area networks would enable tele-medicine to be the solution for future medical treatment of certain conditions [36]. UWB is definitely going to contribute in future evolving technologies like, being integral part of 4G communication, 3D imaging technologies, super complex embedded wireless sensor networks [36] which is shown in Figure 4.1.

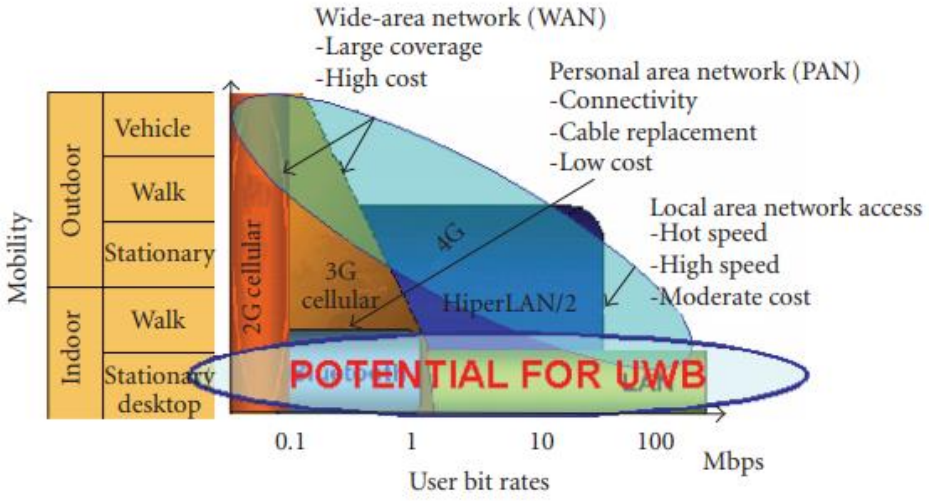


Figure 4.1 Role of UWB in future systems [2].

The work presented in thesis could also be taken on another level by using the UWB measurement on different body types of human. With different body type basically means different fat and protein content in the body and understand how the UWB sensor reacts to such condition [53]. Finally, we plan to conduct research by keeping human subjects in different scenarios like, underground, anechoic, reverberation, office to study the path loss and delay characteristics.

## REFERENCES


[1] Kazimierz Siwiak, Debra McKeown, "Ultra-Wideband Radio Technology", URL: https://onlinelibrary.wiley.com/doi/pdf/10.1002/0470859334.fmatter.

[2] Maria-Gabriella Di Benedetto, Thomas Kaiser, Andreas F. Molish, Ian Oppermann, Christian Politano, Domenico Porcino, "UWB Communication Systems: A Comprehensive Overview",URL: downloads.hindawi.com/books/9789775945105.pdf

[3] Mohammad Monirujjaman Khan, Qammer H. Abbasi, Akram Alomainy, and Yang Hao, "Performance of Ultrawideband Wireless Tags for On-Body Radio Channel Characterisation", URL: http://dx.doi.org/10.1155/2012/232564

[4] A. Fort, C. Desset, P. de Doncker, P. Wambacq, and L. van Biesen, "An ultra-wideband body area propagation channel—from statistics to implementation," IEEE Transactions on Microwave Theory and Techniques, vol. 54, no. 4, pp. 1820–1826, 2006.

[5] A. Fort, C. Desset, J. Ryckaert, P. de Doncker, L. van Biesen, and P. Wambacq,"Characterization of the ultra wideband body area propagation channel," in Proceedings of the IEEE International Conference on Ultra-Wideband (ICU'05), pp. 22–27, September 2005.

[6] A. Alomainy, Y. Hao, X. Hu, C. G. Parini, and P. S. Hall, "UWB on-body radio propagation and system modelling for wireless body-centric networks," *IEE Proceedings: Communications*, vol. 153, no. 1, pp. 107–114, 2006.

[7] Q. H. Abbasi, A. Sani, A. Alomainy, and Y. Hao, "On-body radio channel characterization and system-level modeling for multiband OFDM ultra-wideband body centric wireless network," IEEE Transactions onMicrowave Theory and Techniques,vol. 58, no. 12, pp. 3485–3492, 2010.

[8] Q. Wang and J. Wang, "Performance of on-body chest-towaist UWB communication link," IEEE Microwave and Wireless Components Letters, vol. 19, no. 2, pp. 119–121, 2009.

[9] Q. Wang, T. Tayamachi, I. Kimura, and J. Wang, "An on-body channel model for UWB body area communications for various postures," IEEE Transactions on Antennas and Propagation, vol. 57, no. 4, pp. 991–998, 2009.

[10] A. Sani and Y. Hao, "Modeling of path loss for ultrawide band body-centric wireless communications," in Proceedings of the International Conference on Electromagnetics in Advanced Applications (ICEAA'09), pp. 998–1001, Turin, Italy, September 2009.

[11] T. Zasowski, F. Althaus, M. Stager A, Wittneben, and G. Troster, "UWB for oninvasive wireless body area networks: channel measurements and results," in Proceedings of the IEEE Conference on Ultra Wideband Systems and Technologies, pp. 285–289, November 2003.

[12] A. Alomainy, Y. Hao, C. G. Parini, and P. S. Hall, “Comparison between two different antennas for UWB on-body propagation measurements,” IEEE Antennas and Wireless Propagation Letters, vol. 4, no. 1, pp. 31–34, 2005.

[13] Q. H. Abbasi, A. Sani, A. Alomainy, and Y. Hao, “Arm movements effect on ultra wideband on-body propagation channels and radio systems,” in Proceedings of the Loughborough Antennas and Propagation Conference (LAPC’09), pp. 261–264, Loughborough, UK, November 2009.

[14] A. Alomainy, Q. H. Abbasi, A. Sani, and Y. Hao, “System-level modelling of optimal ultra wideband body-centric wireless network,” in Proceedings of the Asia Pacific Microwave Conference 2009 (APMC’09), pp. 2188–2191, Singapore, December 2009.

[15] A. Sani, G. Palikaras, A. Alomainy, and Y. Hao, “Time domain UWB radio channel characterisation for body-centric wireless communications in indoor environment,” in Proceedings of the IET Seminar on Wideband and Ultrawideband Systems and Technologies: Evaluating Current Research and Development, no. 12352, November 2008.

[16] A. Sani, A. Alomainy, and Y. Hao, “Effect of the indoor environment on the UWB on-body radio propagation channel,” in Proceedings of the 3rd European Conference on Antennas and Propagation (EuCAP’09), pp. 455–458, March 2009.

[17] A. Alomainy, A. Sani, A. Rahman, J. G. Santas, and Y. Hao, “Transient characteristics of wearable antennas and radio propagation channels for ultrawideband body-centric wireless communications,” IEEE Transactions on Antennas and Propagation, vol. 57, no. 4, pp. 875–884, 2009.

[18] Famolari, D., and P. Agarwal, “Architecture and Performance of an Embedded IP PAN,” IEEE ICPWC, 2000.

[19] Stratis, G., S. Sibecas and R. Kipp, “Composite Antenna Pattern for Realistic Ray Tracing Simulations,” IEEE APS International Symposium,2003.

[20] Schwendener, R., “Indoor Radio Channel Model for Protocol Evaluation of Wireless Personal Area Networks,” 13th IEEE International Symposium on Personal, Indoor and Mobile Radio Communications, 2002.

[21] Young-Hoon Kim and Seong-Cheol Kim, "The Effect of Human Bodies on Path Loss Model in an Indoor LOS Environment", URL: http://citeseerx.ist.psu.edu/viewdoc/download?doi=10.1.1.1000.6104&rep=rep1&type=pdf

22] K. P. Burnham and D. R. Anderson, “Model Selection and Multimodel Inference: A Practical Information-Theoretic Approach, Springer”, New York, NY, USA, 2002.

[23] A. Fort, C. Desset, P. de Doncker, P. Wambacq, and L. van Biesen, “An ultra-wideband body area propagation channel model—from statistics to implementation,” IEEE Transactions on Microwave Theory and Techniques, vol. 54, no. 4, pp. 1820–1826, 2006.

[24] L. Yang and G.B. Giannakis, “Ultra-wideband communications: an idea whose time has come,” IEEE Signl.Proc. Mag., Vol. 21, pp. 26 - 54, Nov. 2004.

[25] D. Porcino and W. Hirt, “Ultra-wideband radio technology: potential and challenges ahead,” IEEE Commun.Mag., Vol. 41, pp. 66 - 74, July 2003

[26] J. Blyler, “Location based services are positioned for growth,” Wireless Systems Design Newsletter, Sept. 2003

[27] S. Garg, M. Kappes, and M. Mani, “Wireless access server for quality of service and location based access control in 802.11 networks,” Proc. IEEE Seventh Int. Symp. On Computers and Communications, 1-4 Jul. 2002, pp. 819-824

[28] Oklahoma State University, Richmond Hill lab, Anechoic chamber, URL: https://reverb.okstate.edu/sites/default/files/slideshow-images/Anechoic.JPG

[29] Federal Communications Commission, “First report and order 02-48,” tech. rep., 2002

[30] A brief history of UWB communication, URL: http://ptgmedia.pearsoncmg.com/images/chap1_0131463268/elementLinks/01fig01.gif

[31] Hall, P.S., Hao, Y.: ‘Antennas and propagation for body-centric wireless communications’ (Artech House, 2006)

[32] Kolmogorov–Smirnov test, URL: https://en.wikipedia.org/wiki/Kolmogorov%E2%80%93Smirnov_test

[33] Anderson Darling test, URL: https://en.wikipedia.org/wiki/Anderson%E2%80%93Darling_test

[34] Anderson Darling test, URL: https://www.itl.nist.gov/div898/handbook/eda/section3/eda35e.htm

[35] Smith, Julius O. Spectral Audio Signal Processing,W3K Publishing, http://books.w3k.org/,ISBN 978-0-9745607-3-1.

[36] Ben Allen, Tony Brown, Katja Schwieger, Ernesto Zimmermann, Wasim Malik, David Edwards, Laurent Ouvry, Ian Oppermann, (2005), Ultra Wideband: Applications, Technology and Future perspectives, The International Workshop on convergent technologies (IWCT), Oulu,Finland, URL: http://hdl.handle.net/10547/269833.

[37] Subdomain of body centric communication, URL: http://medsmagazine.com/wp-content/uploads/2012/01/MEDS4-STMicro-Fig1-550x389.jpg

[38] Rappaport, Theodore S. "Wireless Communications -- Principles and Practice, Second v Edition. (The Book End)." Microwave Journal, Dec. 2002, p. 128. Academic OneFile, http://link.galegroup.com/apps/doc/A97115718/AONE?u=tcc_trial&sid=AONE&xid=a6e80ed6. Accessed 17 Apr. 2018.

[39] Andrea Goldsmith, “WIRELESS COMMUNICATIONS”, URL: http://web.cs.ucdavis.edu/~liu/289I/Material/book-goldsmith.pdf

[40] Basic antenna communication, URL: http://rfandwireless.com/5/wp-content/uploads/2016/04/1-3.jpg

[41] Zoubir Irahhauten, Homayoun Nikookar, and Gerard J. M. Janssen, "An Overview of Ultra Wide Band Indoor Channel Measurements and Modeling", URL: http://citeseerx.ist.psu.edu/viewdoc/download?doi=10.1.1.331.8198&rep=rep1&type=pdf.

[42] On-body communication, URL : https://en.wikipedia.org/wiki/On-body_wireless

[43] C. G. Spiliotopoulos and A. G. Kanatas, "Channel measurements and modelling in a military cargo airplane," *Progress In Electromagnetics Research B*, Vol. 26, 69-100, 2010.

[44] Khan, M. M., Abbasi, Q. H., Alomainy, A., Hao, Y., & Parini, C. (2013). Experimental characterisation of ultra-wideband off-body radio channels considering antenna effects. IEE Proceedings.Microwaves, Antennas and Propagation., 7(5), 370-380. Retrieved from http://argo.library.okstate.edu/login?url=https://search.proquest.com/docview/1492899294?accountid=4117

[45] Johan Karedal, Shurjeel Wyne, Peter Almers, Fredrik Tufvesson, and Andreas F. Molisch, "UWB Channel , Measurements in an Industrial Environment", URL: https://ieeexplore.ieee.org/stamp/stamp.jsp?tp=&arnumber=1379019.

[46] Nobles, Phil & Ashworth, D & Halsall, F. (1994). Indoor radiowave propagation measurements at frequencies up to 20 GHz. 873 - 877 vol.2. 10.1109/VETEC.1994.345215.

[47] Z. Irahhauten, H. Nikookar and G. J. M. Janssen, "An overview of ultra wide band indoor channel measurements and modeling," in *IEEE Microwave and Wireless Components Letters*, vol. 14, no. 8, pp. 386-388, Aug. 2004.

[48] Rusch, Leslie & Prettie, Cliff & Cheung, David & Li, Qinghua & Ho, Minnie. (2003). Characterization of UWB Propagation from 2 to 8 GHz in a Residential Environment. IEEE Journal on Selected Areas in Communications - JSAC.

[49] S. S. Ghassemzadeh, R. Jana, C. W. Rice, W. Turin and V. Tarokh, "Measurement and modeling of an ultra-wide bandwidth indoor channel," in *IEEE Transactions on Communications*, vol. 52, no. 10, pp. 1786-1796, Oct. 2004.

[50] Mohammad Monirujjaman Khan, Qammer H. Abbasi, Akram Alomainy, and Yang Hao, "Performance of Ultrawideband Wireless Tags for On-Body Radio Channel Characterisation," International Journal of Antennas and Propagation, vol. 2012, Article ID 232564, 10 pages, 2012.

[51] V. Erceg, L. J. Greenstein, S. Y. Tjandra, S. R. ParkOff, A. Gupta, B. Kulic, A. A. Julius, and R. Bianchi, "An empirically based path loss model for wireless channels in suburban environments," *IEEE Journal on Selected Areas in Communications*, pp. 1205–1211, July 1999.

[52] Vector Network Analyzer, URL: https://en.wikipedia.org/wiki/Network_analyzer_(electrical)

[53] T. Kumpuniemi, M. Hämäläinen, K. Y. Yazdandoost and J. Iinatti, "Measurements for body-to-body UWB WBAN radio channels," 2015 9th European Conference on Antennas and Propagation (EuCAP), Lisbon, 2015, pp. 1-5.

.

VITA

Surbhi Vishwakarma

Candidate for the Degree of

Master of Science

Thesis: ULTRA-WIDEBAND CHANNEL MEASUREMENT AND MODELING FOR UNMANNED AERIAL VEHICLE TO WEARABLE COMMUNICATION

Major Field: Electrical and Computer Engineering

Biographical:

Education:

Completing the requirements for the Master of Science in Electrical and Computer Engineering at Oklahoma State University, Stillwater, Oklahoma in May, 2018.

Completed the requirements for the Bachelor of Science in Electronics and Communication Engineering at Vellore Institute of Technology, Vellore in 2015.

Experience:

Research Assistant, Oklahoma State University, Stillwater, OK

Summer Research, National Aeronautics and Space Administration (NASA)

Student tutor at LASSO tutoring center, Oklahoma State University

Project Associate, Indian Institute of Technology, Madras.

Summer Internship, Indian Institute of Technology, Gandhinagar

Professional Memberships:

Program Chair, Automation Society, Oklahoma State University

Cultural Secretary, Indian Student Association

Student Liaison, GPSGA Organization